

What types of chemical problems benefit from density-corrected DFT? A probe using an extensive and chemically diverse test suite

*Golokesh Santra and Jan M.L. Martin**

Department of Organic Chemistry, Weizmann Institute of Science, 7610001 Rehovot, Israel.

Email: gershom@weizmann.ac.il

Abstract

For the large and chemically diverse GMTKN55 benchmark suite, we have studied the performance of density-corrected density functional theory (HF-DFT), compared to self-consistent DFT, for several pure and hybrid GGA and meta-GGA exchange-correlation (XC) functionals (PBE, BLYP, TPSS, SCAN) as a function of the percentage of HF exchange in the hybrid. The D4 empirical dispersion correction has been added throughout. For subsets dominated by dynamical correlation — particularly noncovalent interaction subsets — HF-DFT is highly beneficial, particularly at low HF exchange percentages. For subsets with significant static correlation (i.e., where a Hartree-Fock determinant is not a good zero-order wavefunction), HF-DFT may do more harm than good. While the self-consistent series show optima at or near 37.5% (i.e., 3/8) for all four XC functionals — consistent with Grimme’s proposal of the PBE38 functional — HF-B n LYP-D4, HF-PBE n -D4, and HF-TPSS n -D4 all exhibit minima nearer 25% (i.e., 1/4). Intriguingly, for HF-SCAN n -D4, the minimum is near 10%, but the weighted mean absolute error (WTMAD2) for GMTKN55 is only barely lower than that of HF-SCAN-D4 (i.e., where the post-HF step is a pure meta-GGA). The latter becomes an attractive option, only slightly more costly than pure Hartree-Fock, and devoid of adjustable parameters other than the three in the dispersion correction. Moreover, its WTMAD2 is only surpassed by the highly empirical M06-2X and by the combinatorically optimized empirical range-separated hybrids ω B97X-V and ω B97M-V.

Introduction

In a review with the provocative title, “The importance of being inconsistent,” Burke, Wasserman, Sim, et al.,¹ give an overview of the HF-DFT method, also known as the DC-DFT (for density-corrected DFT) method. The essential stratagem of HF-DFT actually goes back to the dawn of molecular DFT, where — as a pragmatic expedient that permitted quickly retrofitting DFT into a wavefunction *ab initio* program system — new GGA or mGGA exchange-correlation functionals would be evaluated for densities generated from pure Hartree-Fock SCF orbitals.^{2,3} (A related practice, “post-LDA DFT,” consisted of using LDA densities from early DFT codes in the same fashion,⁴ so a new GGA or meta-GGA functional could quickly be assessed before going to the trouble of a self-consistent implementation.)

Pure HF orbitals are rigorously free of self-interaction error (SIE). While, for instance, PBE evaluated using HF orbitals will not be SIE-free, Lonsdale and Goerigk observed⁵ that HF-DFT functionals systematically have lower SIE than the corresponding self-consistent functional.

More generally speaking, HF-XC (where XC is a given exchange-correlation functional) arguably might be beneficial in any situation where the chief source of error in XC is a misshapen density, rather than intrinsic exchange and correlation errors.

Very recently, Burke and coworkers found^{6,7} that HF-DFT is beneficial in the treatment of halogen and pnictogen bonds. As we have some experience in halogen bonding (e.g.,^{8,9}) we were intrigued by this finding. We were also motivated in part by our work on minimally empirical double hybrids,^{10,11} and by the question whether HF-DFT would still be beneficial at the high percentages of Hartree-Fock exchange such functionals typically entail.

It then occurred to us that, to our knowledge, no evaluation had yet been carried out of HF-DFT with a large and chemically diverse benchmark suite like GMTKN55 (general main-group thermochemistry, kinetics, and noncovalent interactions—55 problem types¹²). We present such an analysis below for several hybrid GGA and meta-GGA sequences, with percentages of Hartree-Fock exchange in the functional varying from 0 to 50%.

We also ought to point out an interesting parallel, from a wavefunction theory perspective, between HF-DFT and the proposed separation between static and dynamical correlation originally proposed by Cioslowski¹³ and developed into a static correlation diagnostic by Matito and coworkers:¹⁴

$$E_{\text{HF}}[\rho_{\text{HF}}] \rightarrow E_{\text{FCI}}[\rho_{\text{HF}}] \rightarrow E_{\text{FCI}}[\rho_{\text{FCI}}]$$

Where the first step corresponds to dynamical and the second to static correlation. It is hard not to see the parallel with

$$E_{\text{HF}}[\rho_{\text{HF}}] \rightarrow E_{\text{XC}}[\rho_{\text{HF}}] \rightarrow E_{\text{XC}}[\rho_{\text{XC}}]$$

In which XC is an exchange-correlation functional. The first step corresponds to HF-DFT; in the (hypothetical) scenario that XC would capture dynamical correlation exactly, then HF-XC would approach exactitude for systems dominated by dynamical correlation.

The analogy goes only so far, of course — self-interaction error, for instance, is a non-issue with wavefunction methods.

Computational Details

The GMTKN55 (General Main-group Thermochemistry, Kinetics, and Noncovalent Interactions, 55 problem sets) benchmark suite of Goerigk, Grimme, and co-workers¹² was used as our validation set. This dataset consists of nearly 1500 energy differences entailing almost 2500 energy evaluations. Its 55 subsets can be conveniently grouped into five classes: thermochemistry, barrier heights, intermolecular (noncovalent) interactions, conformers (dominated by *intramolecular* noncovalent interactions), and reaction energies for large systems. A detailed description of all 55 subsets can be found in the original paper,¹² and a brief itemized summary in the present paper's ESI (electronic supporting information).

As our primary error metric, we used the WTMAD2 (weighted mean absolute deviation, type 2 as defined in the original GMTKN55 paper¹²): its expression has the form

$$\text{WTMAD2} = \frac{1}{\sum_{i=1}^{55} N_i} \cdot \sum_{i=1}^{55} N_i \cdot \frac{56.84 \text{ kcal/mol}}{|\overline{\Delta E}|_i} \cdot \text{MAD}_i$$

Where the $|\overline{\Delta E}|_i$ are the mean absolute values of all the reference energies for subset $i = 1$ to 55 (thus 'normalizing' errors of all subsets to the same scale, so to speak), N_i is the number of systems in subset i , and MAD_i represents the mean absolute difference between our calculated and the original reference energies for subset i . We also considered the WTMAD2 contributions for the five primary categories, as well as for the individual subsets.

The primary reason, in Ref.¹² and in the present work, to choose an MAD-based metric over an RMSD (root mean square deviation)-based one, is that MAD is a more 'robust' in the

statistical sense¹⁵ (e.g., less prone to strongly vary because of one or two outliers). The RMSD/MAD ratio for an unbiased normal distribution should be¹⁶ $(\pi/2)^{1/2}=1.253314\dots\approx 5/4$; an abnormally large or small ratio is almost invariably an indicator for outliers. Hence, we monitored the RMSD/MAD ratio for each subset throughout the work.

Our first HF-DFT explorations (involving PBE hybrids) were carried out using the Gaussian16 package,¹⁷ the remainder using ORCA 4.2.1,¹⁸ all running on the Faculty of Chemistry's CHEMFARM high-performance computing facility. Some additional calculations were carried out using Q-CHEM.¹⁹

Reference geometries from Ref.¹² were used as-is, without any further optimization. For most of the systems in HF-DFT and SC-DFT single point electronic structure calculations, the Weigend–Ahlrichs def2-QZVPP²⁰ basis set was used, except for the five anion-containing subsets WATER27, RG18, IL16, G21EA, and AHB21 where we used diffuse-function augmented def2-QZVPPD.²¹ Density fitting for the Coulomb and exchange part was used throughout in ORCA, in conjunction with the appropriate def2/JK density fitting basis sets.²² In the ORCA calculations, we employed GRID 5 as the integration grid, except for the SCAN (strongly constrained and appropriately normed²³ [nonempirical] meta-GGA functional) and HF-SCAN series, where we used the larger GRID 6 because of SCAN's well-documented²⁴ strong integration grid sensitivity. TightSCF convergence criteria were used throughout. In Q-Chem, we used the SG-3 grid²⁵ throughout. (Sample HF-DFT inputs for Gaussian16 and ORCA can be found in the ESI.)

One series of calculations, HF-PBE n , consisted of HF-DFT counterparts of PBE²⁶ (0% HF exchange), PBE0²⁷ (25% HF exchange), PBE38²⁸ (37.5% HF exchange) and PBE50²⁹ (50% HF exchange), as well as the respective self-consistent functionals for comparison. A second was HF-B n LYP, consisting of HF-DFT versions of BLYP^{30,31} (0% HF exchange), B3LYP³² (20% HF exchange[†]), B1LYP³³ (25% HF exchange), B38LYP (37.5% HF exchange), and BHLYP^{31,34} (50% HF exchange), again compared with their self-consistent variants. We briefly discuss a third series comprising HF-DFT and self-consistent DFT versions of the meta-GGA TPSS³⁵ (0% HF exchange), TPSSh (10% HF exchange),³⁶ TPSS0 (25% HF exchange), TPSS38 (37.5% HF exchange), and TPSS50 (50% HF exchange). Finally, we explore HF-DFT and self-consistent series of the recent SCAN meta-GGA functional:²³ SCAN (0% HF exchange), SCAN10 (10% HF exchange), SCAN0 (25% HF exchange), SCAN38 (37.5% HF exchange), and SCAN50 (50% HF exchange).

[†] B3LYP, unlike the others, uses a mix of 8% Slater LSDA and 72% Becke88 exchange,⁸¹ and a mix of 19% VWN5 LSDA correlation⁸² + 81% LYP GGA correlation³¹

In order to treat dispersion on an equal footing everywhere, the recent DFT-D4 model,^{37,38} as implemented in Grimme’s standalone `dftd4` program (<https://www.chemie.uni-bonn.de/pctc/mulliken-center/software/dftd4>), was employed throughout. Since not for all self-consistent cases “official” parameters were available, and none at all were available for HF-DFT-D4, we refitted the three nontrivial parameters s_8 , a_1 , and a_2 for each functional by minimizing WTMAD2 over GMTKN55. (As we do not consider double hybrids^{11,39} in the present work, the fourth parameter is constrained to be $s_6=1$ throughout, as is the prefactor for the 3-body Axilrod-Teller-Muto^{40,41} correction, $c_{\text{ATM}}=1$.) The D4 parameter optimizations were performed using Powell’s derivative-free constrained optimizer, BOBYQA (Bound Optimization BY Quadratic Approximation)⁴² and a collection of scripts developed in-house.

All parameter values, and the corresponding WTMAD2s and five-component breakdowns of same, can be found in Table S2 in the ESI, where the corresponding data for any available ‘official’ parametrizations are also given.

Results and Discussion

(a) GGA series: PBE n -D4 vs. HF-PBE n -D4 and BnLYP-D4 vs. HF-BnLYP

Our discussion will focus mostly on the PBE n -D4 vs. HF-PBE n -D4 series, but behavior of the BnLYP-D4 vs. HF-BnLYP-D4 series (see Supporting Information) is, by and large, quite similar. In Figure 1 we summarize, for all four scenarios, the dependence on the percentage of HF exchange of WTMAD2 as well as of its five top-level subdivisions: basic thermochemistry (THERMO), reaction barrier heights (BARRIER), large-molecule reactions including isomerizations (LARGE), conformational equilibria (CONFOR) — which are generally driven by intramolecular noncovalent interactions — and intermolecular interactions (INTER).

Intriguingly, for both PBE n -D4 and BnLYP-D4, the overall minimum is not near 25% as one might expect,⁴³ but near 37.5% or 3/8, consistent with the PBE38 functional proposed by Grimme and coworkers.^{28,44} The minor loss in accuracy for basic thermochemistry is more than compensated by the improvements for barrier heights and for large-molecule isomerization reactions. In contrast, HF-PBE n -D4 and HF-BnLYP-D4 see WTMAD2 minima at lower percentages of HF exchange, closer to 25% or 1/4 in the PBE case, and to 30% in the BLYP case. (It has been well known for over two decades⁴⁵⁻⁴⁷ that barrier heights of radical reactions are systematically underestimated by GGAs and that hybrids with high percentages of HF exchange (e.g.^{47,48}) yield the best performance. This has been ascribed⁴⁹⁻⁵¹ to self-interaction error — which is reduced as the percentage of HF exchange is increased — and it has been shown convincingly (e.g., Refs.^{51,52}) that barrier predicted by (meta)GGAs are much improved by self-interaction corrections or, to a lesser extent, by HF-DFT.⁵³ In some situations, however, such as pnictogen inversion

barriers, HF exchange counterintuitively lowers barriers,⁵⁴ which has been rationalized by Mahler et al.⁵⁵ as occurring in situations where bond orbitals in the transition state have more s and less p character than in reactants and products.)

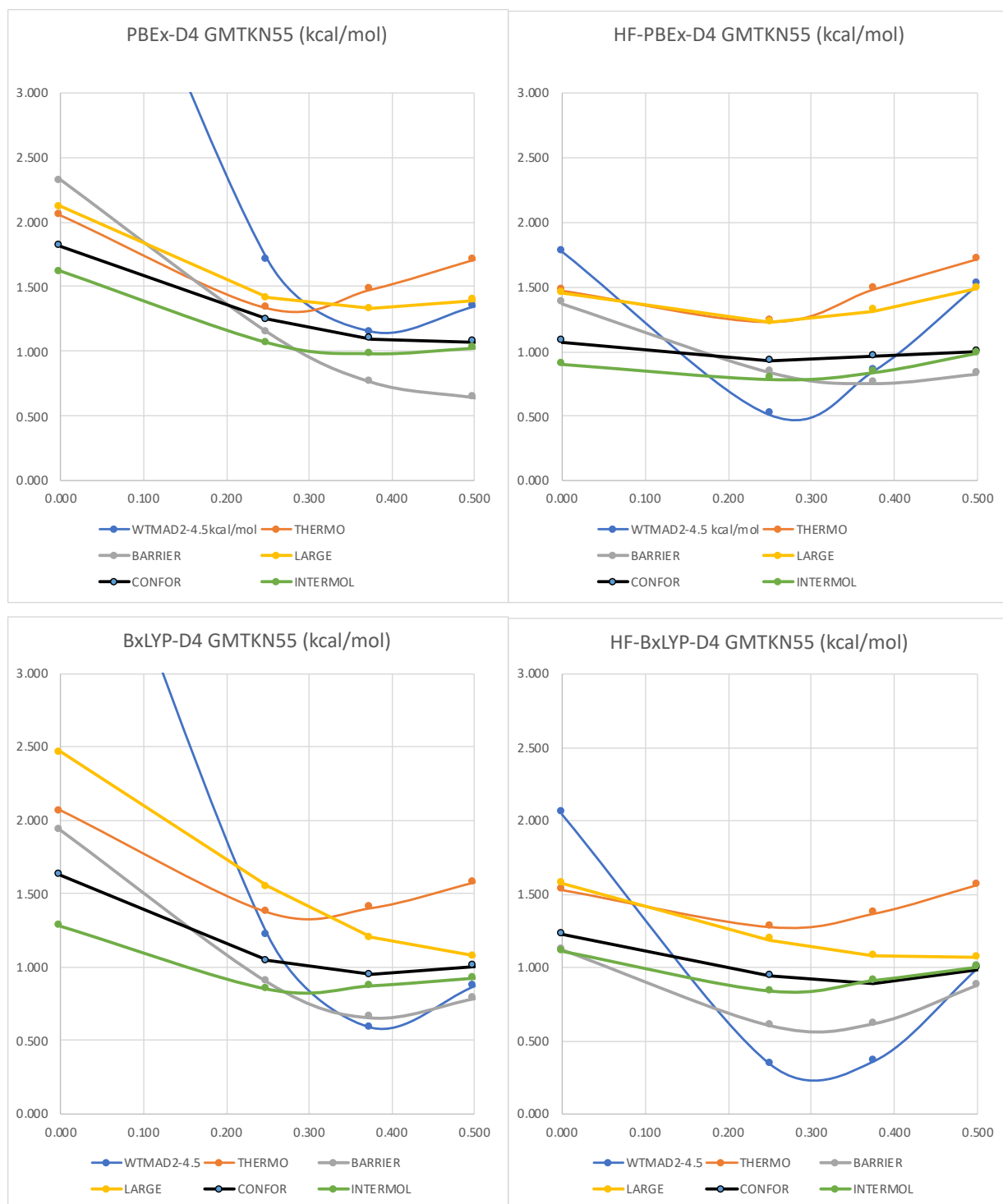


Figure 1: Dependence of WTMAD2 (kcal/mol) and of the five top-level subsets on the percentage of HF exchange (x axis) for PBE n -D4, HF-PBE n -D4, B n LYP-D4, and HF-B n LYP-D4

The gain from using HF orbitals is greatest for $n=0$, namely 3.64 kcal/mol for HF-PBE-D4 and 2.81 kcal/mol for HF-BLYP-D4. It is still significant for HF-PBE0-D4, -1.19 kcal/mol, and HF-B1LYP-D4, -0.88 kcal/mol. Then it continues to decay monotonically until it becomes a net liability for HF-BHLYP-D4 and HF-PBE50-D4.

Breaking down by the five top-level components, we see that HF-PBE n -D4 nearly ‘flattens the curves,’ compared to PBE n -D4, for conformers and intermolecular interactions. In the low-HF region, barrier heights benefit most significantly, but this vanishes around HF-PBE38-D4: self-consistent densities with high percentages of HF exchange still do better.

Benefits are seen at zero to moderate HF exchange for large-molecule reactions and for basic thermochemistry.

For the B n LYP series, the curves for conformers and intermolecular interactions are flatter to begin with, presumably because LYP is a very short-ranged correlation functional and dispersion corrections play a much larger role here. (By way of illustration: for the simple D2 empirical dispersion correction, which just has a simple scaling factor s_6 as an empirical parameter, $s_6=0.65$ for PBE0 and 1.2 for B3LYP.⁵⁶) Otherwise, things are much the same as for the PBE series: HF-DFT definitely is beneficial at zero to moderate (about 25%) HF exchange, and becomes detrimental overall at 50% HF exchange.

Let us now zoom in on individual subsets that vary the most (Figure 2). First, the SIE4x4 self-interaction subset benefits for all percentages of HF exchange, reducing it by 10-25%.

The BH76 subset of 76 barrier heights is the set union of Truhlar’s HTBH38 and NHTBH38 hydrogen- and non-hydrogen transfer barrier heights.^{57,58} Here, the improvement granted by HF-DFT is quite dramatic at zero or low HF exchange — at 50% HF-DFT is actually detrimental, while at 37.5% it is a wash. For the PX13 proton exchange barriers, we again see a substantial benefit at 0% and a significant one at 25%. Intriguingly, for the BHPERI pericyclic reactions, HF-DFT appears to be detrimental — but this may be masked by the known fact⁵⁹ that dispersion contributions — which disproportionately stabilize the transition states — are quite significant for these barriers.

For the HAL59 halogen bonds, the PNICO23 pnictogen bonds, and the WATER27 water clusters (multiple hydrogen bonds), HF-PBE n -D4 is beneficial across the board, while for the B n LYP series — where the contribution of the D4 dispersion correction is larger — we actually find that HF-B n LYP-D4 is detrimental for WATER27 but beneficial for higher percentages of HF exchange: B n LYP-D4 underbinds on average for 0% but overbinds for the other, and HF-B n LYP lowers the interaction energies.

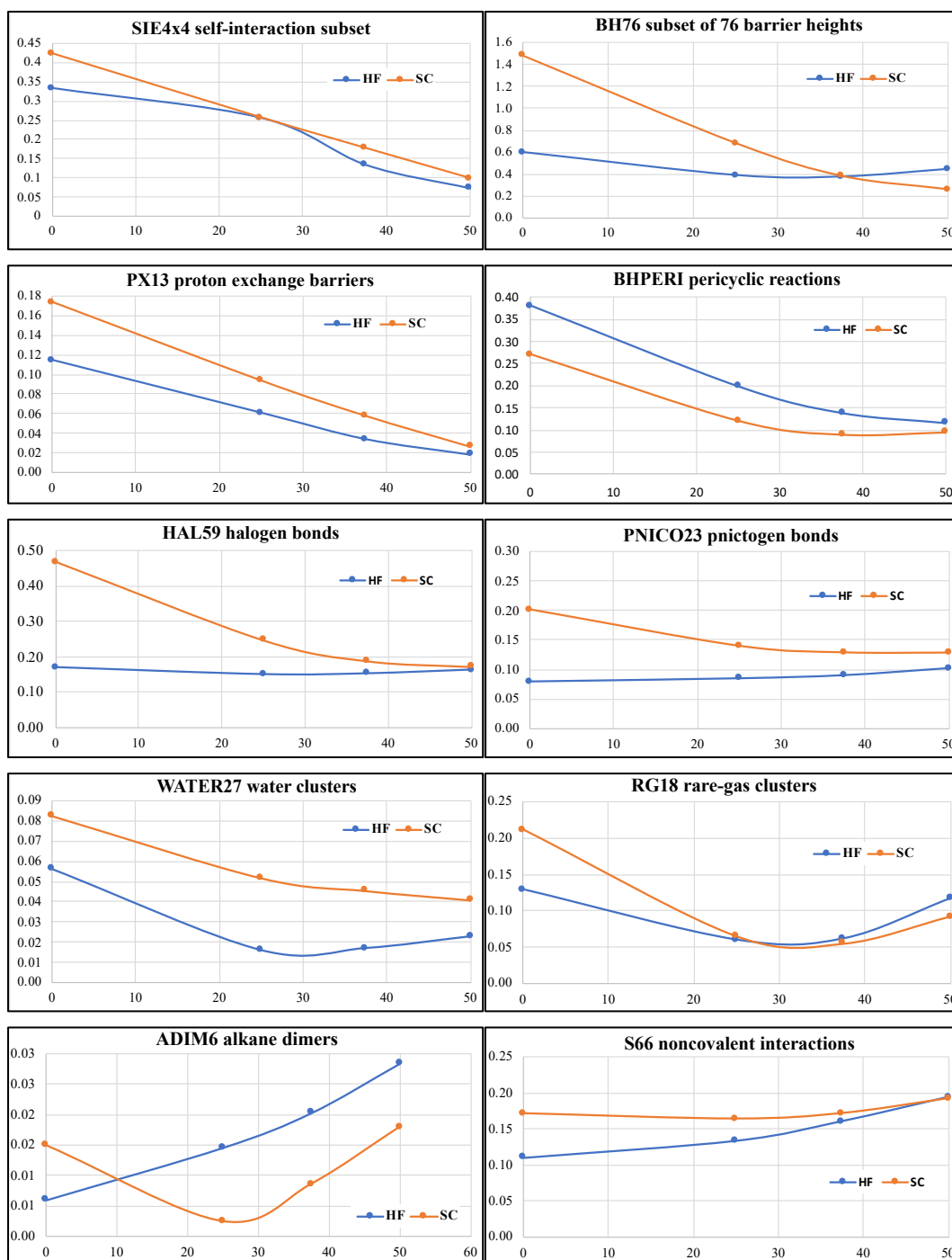


Figure 2: Dependence on the percentage of HF exchange, for self-consistent PBE-D4 (SC) and HF-PBE-D4 (HF) of the WTMA D2 (kcal/mol) contributions for the individual subsets SIE4x4, BH76, PX13, BHPERI, HAL59, PNICO23, WATER27, RG18, ADIM6, S66, alkane conformers(ACONF), 1,4-butanediol conformers(BUT14DIOL), oligopeptide conformers (PCONF21), sugar conformers(SCONF), amino acid conformers(AMINO20X4), G21EA, W4-11, DC13 and large molecule isomerization(ISOL24) subsets. A similar figure for the BnLYP-D4 and HF-BnLYP-D4 cases appears as Figure S1 in the ESI.

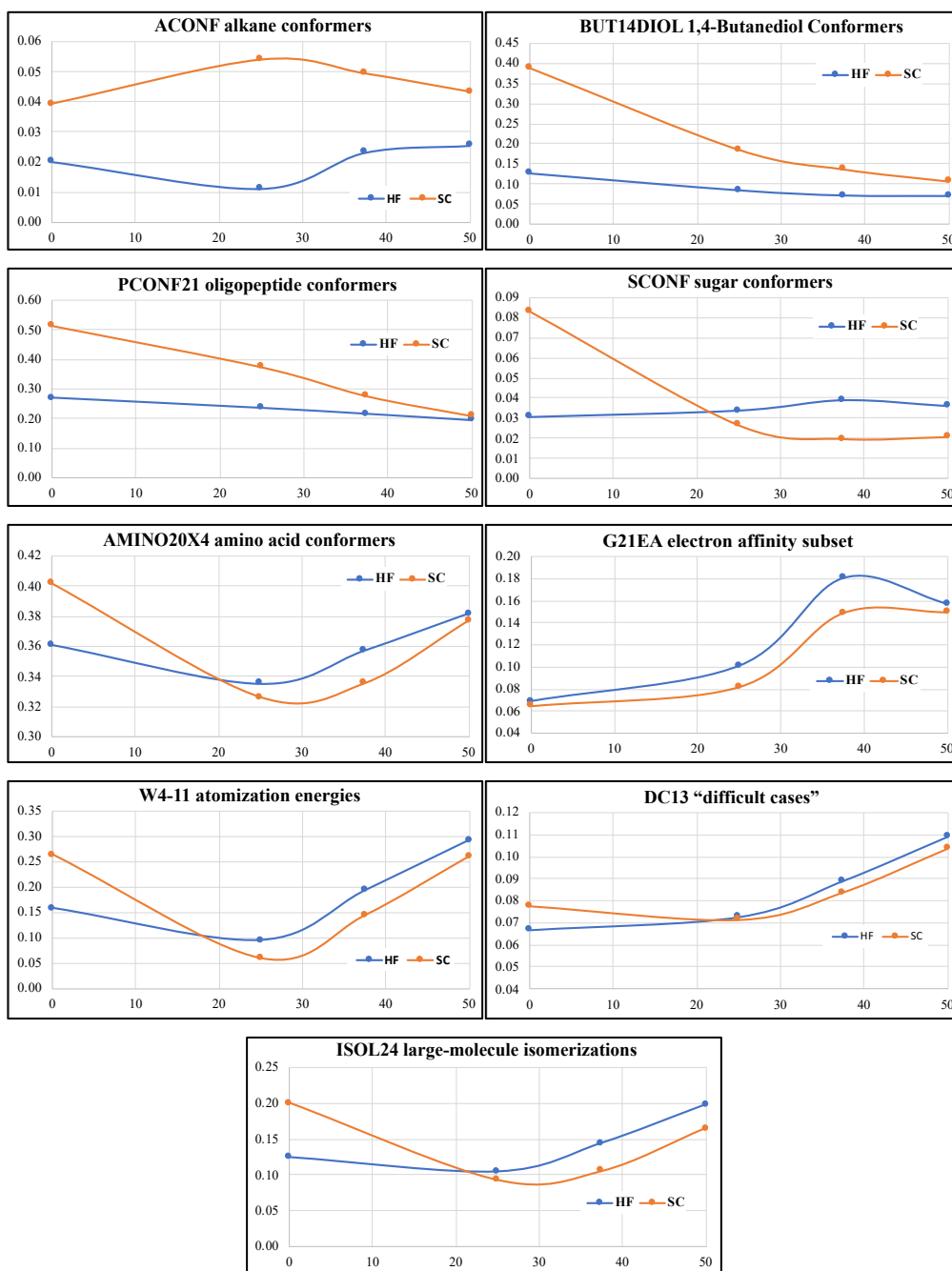


Figure 2 (continued)

From a symmetry-adapted perturbation theory (SAPT) point of view,⁶⁰ the three sets above have in common that they are predominantly driven by electrostatic interactions rather than dispersion. So, what about dispersion-dominant subsets? The RG18 rare-gas clusters and the ADIM6 n-alkane dimers are archetypical examples: in neither is HF-DFT very helpful, which makes sense since the interactions occur at a longer distance.

The S66 noncovalent interactions benchmark⁶¹ (see Ref.⁶² for a recent revision) is a more mixed bag. Breaking down by subsets reveals the answer here: systems 1-23 are hydrogen bonds, 24 through 33 π -stacking, 34 through 46 London dispersion complexes, and the remainder mixed-influence. Again, we see that HF-DFT is beneficial mostly for the hydrogen bond component: this is most pronounced for the PBE series (Table 1).

Table 1: MAD (kcal/mol) values of four subcategories and full S66 set for both PBE & PBE n -D4 and BLYP & B n LYP-D4 variants.

Functionals	Hydrogen Bonds Sys. 1-23	π -stacking Sys. 24-33	London Dispersion Sys. 34-46	Mixed-influence Systems 47-66	Full S66 set
HF-PBE-D4	0.198	0.442	0.182	0.223	0.240
PBE-D4	0.594	0.397	0.312	0.150	0.374
HF-PBE0-D4	0.342	0.315	0.223	0.261	0.290
PBE0-D4	0.601	0.260	0.310	0.208	0.373
HF-PBE38-D4	0.481	0.286	0.251	0.293	0.349
PBE38-D4	0.694	0.139	0.182	0.247	0.374
HF-PBE50-D4	0.670	0.198	0.307	0.327	0.423
PBE50-D4	0.785	0.103	0.192	0.293	0.416
HF-BLYP-D4	0.221	0.147	0.760	0.350	0.355
BLYP-D4	0.203	0.477	0.407	0.351	0.330
HF-B3LYP-D4	0.260	0.114	0.565	0.187	0.276
B3LYP-D4	0.491	0.361	0.219	0.121	0.306
HF-B1LYP-D4	0.328	0.150	0.571	0.189	0.307
B1LYP-D4	0.494	0.210	0.356	0.159	0.322
HF-BHLYP-D4	0.995	0.263	0.241	0.282	0.519
BHLYP-D4	1.063	0.238	0.250	0.265	0.536

Turning now to conformers, in light of the above it is not surprising that a series like the 1,4-butanediol conformers⁶³ — the conformer equilibria of which are dominated by the making and breaking of internal hydrogen bonds — would benefit from HF-DFT. So do sugar and oligopeptide conformers at the low-HF exchange end. Nevertheless, alkane conformers also benefit slightly. Amino acid conformers^{64,65} are a mixed bag, as the equilibria for residues with hydrophobic side chains (e.g., valine, isoleucine, and leucine) will be driven more by dispersion, and those for residues like lysine and arginine more by electrostatics.

In principle, electron affinities should get better, at least for pure BLYP and PBE, because in HF-PBE, the anion HOMO is at least bound. In practice, Tschumper and Schaefer⁶⁶ already showed back in 1997 that because of spatial confinement by the finite basis set, even BLYP and PBE EAs are fairly reasonable. (See also de Oliveira et al.⁶⁷ for more discussion.)

In the present work, we see no improvement in actual EAs from using HF-DFT, and for hybrid functionals HF-DFT actually seems to do more harm than good.

For the W4-11 set of atomization energies,⁶⁸ HF-BLYP-D4 and HF-PBE-D4 are definitely superior over the pure-DFT BLYP-D4 and PBE-D4 functionals, respectively, but with some HF exchange introduced at the orbital stage, self-consistency seems to be more beneficial. Likewise, for the DC13 “difficult cases” benchmark, HF-BLYP-D4 and HF-PBE-D4 are helpful, but here a benefit is seen all along the Bn LYP series. Intriguingly, the large-molecule isomerizations exhibit the same behavior.

(b) *meta-GGA series, particularly HF-SCAN n -D4 vs. SCAN n -D4:*

But perhaps the above behaviors might not carry over well to meta-GGAs such as TPSS. So, we carried out a similar investigation for the HF-TPSS n -D4 and TPSS n -D4 series. Detailed results can be found in the supporting information, but the bottom line is that HF-TPSS n -D4 behaves quite similarly to the HF-PBE n -D4 and HF- Bn LYP-D4 series.

The recent SCAN functional, however, breaks the mold to some degree (Figure 3). The graph for self-consistent SCAN n -D4 qualitatively looks fairly similar to its counterparts for PBE n -D4, Bn LYP-D4, and TPSS n -D4: it even has the same overall minimum at or near 37.5% (3/8) of HF exchange.

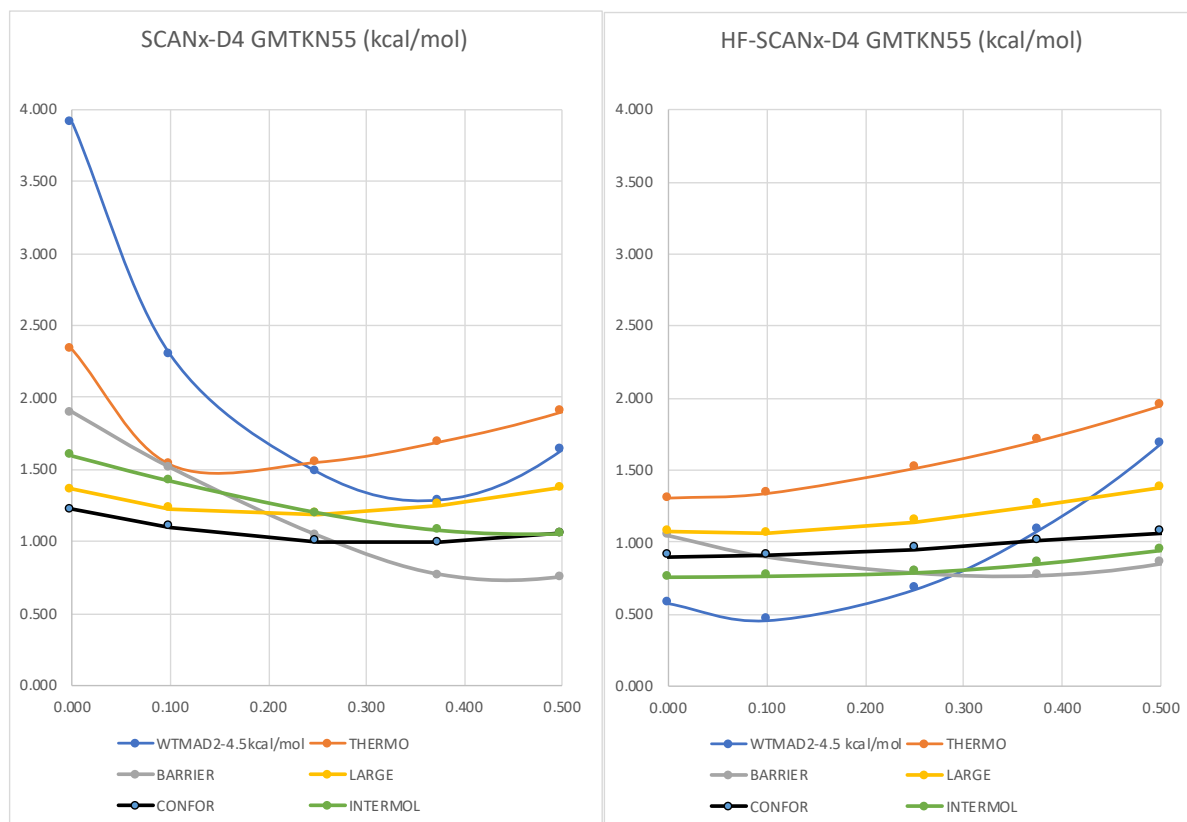


Figure 3: dependence of WTMAD2 (kcal/mol) and of the five top-level subsets on the percentage of HF exchange for HF-SCAN n -D4 and SCAN n -D4,

But when HF orbitals are used, the minimum shifts not to 25% (1/4) as for the abovementioned series, but to about 10%. What is more, HF-SCAN-D4 without any “exact” exchange in the post-HF step performs nearly as well as the “optimum” HF-SCAN10-D4. Comparing this to the compilation of WTMAD2 values for other DFT functionals,^{11,69} (or, with slightly different basis set choices, in Refs. ^{12,70}), the WTMAD2 of 5.08 kcal/mol is superior to all hybrid GGAs and meta-GGAs except for highly parametrized range-separated hybrids like wB97X-V and wB97M-V.^{71,72} It must be emphasized that, aside from the three parameters of the D4 dispersion correction, the HF-SCAN-D4 functional has no adjustable parameters. (The fitted D4 parameters can be found in Table S2 in the ESI.) It will be more attractive in terms of computational cost than other hybrid meta-GGAs, since the cost will basically be that of a simple HF calculation followed by a single evaluation of the SCAN meta-GGA functional.

How is HF-SCAN achieving this quite remarkable result? If we look at the five top-level subclasses of GMTKN55, we find that HF-SCAN n -D4 nearly flattens the intermolecular interaction curve, and improves across the board — especially for lower HF fractions. For conformer energy differences (mainly driven by intramolecular noncovalent interactions), HF-SCAN n -D4 flattens and improves at low HF exchange, while neither helping nor harming much at high HF exchange. By and large, the same is observed for large-molecule reaction energies. For small-molecule thermochemistry, a noticeable improvement is seen at low HF exchange, leading to HF-SCAN-D4 indeed becoming the optimum for that subset. Only for barrier heights is a minimum still found at a high fraction of exact exchange (at or near HF-SCAN38-D4) — but the curve is much flatter than for the SCAN n -D4 series, and indeed for the other HF-functional-D4 series we have considered above.

Now if we focus on individual subsets (Figure S2 in ESI), for the SIE4x4 self-interaction subset benefits are seen up to 50% HF exchange, beyond which self-consistent SCAN n -D4 and HF-SCAN n -D4 perform similarly. BH76, BHPERI, and PX13 exhibit similar trends as the other tested GGA and meta-GGA cases.

In the cases of HAL59, PNICO23 and WATER27, HF variants perform better than the self-consistent counterparts, with (as expected) the performance gap monotonically decreasing as HF exchange is progressively introduced into the DFT part.

For the rare gas interactions subset RG18, HF-SCAN-D4 is quite beneficial over SCAN-D4, but as HF exchange is introduced in the DFT parts, the self-consistent variants “catch up” so that already HF-SCAN0-D4 and SCAN0-D4 have similarly low error statistics. In contrast, for the n-alkane dimer interaction subset ADIM6 — which should likewise be

driven mostly by London dispersion — self-consistent SCAN n -D4 is consistently superior to HF-SCAN n -D4, although both improve as n is increased (unlike the behavior for the PBE series).

For the noncovalent interaction subset S66, HF-SCAN n -D4 outperforms its self-consistent counterpart across the range. Breakdown by subsets reveals this is entirely driven by the hydrogen bonds, the π -stacks and London subsets actually show deterioration when using HF rather than self-consistent densities, while for the mixed-influence complexes, it does not seem to matter which. (Table 2)

Table 2: MAD (kcal/mol) values of four subcategories and full S66 set for HF-SCAN n -D4 and SCAN n -D4

Functionals	Hydrogen Bonds Sys. 1-23	π -stacking Sys. 24-33	London Dispersion Sys. 34-46	Mixed-influence Systems 47-66	All S66set
HF-SCAN-D4	0.209	0.567	0.468	0.225	0.319
SCAN-D4	0.733	0.100	0.344	0.228	0.407
HF-SCAN10-D4	0.308	0.443	0.438	0.241	0.334
SCAN10-D4	0.786	0.079	0.230	0.204	0.393
HF-SCAN0-D4	0.446	0.258	0.415	0.255	0.353
SCAN0-D4	0.838	0.082	0.165	0.234	0.408
HF-SCAN38-D4	0.594	0.148	0.374	0.275	0.386
SCAN38-D4	0.893	0.099	0.141	0.265	0.434
HF-SCAN50-D4	0.790	0.134	0.275	0.323	0.448
SCAN50-D4	0.985	0.097	0.113	0.321	0.477

1,4-butanediol conformers BUT14DIOL systematically benefit from HF densities, although the gap with self-consistent SCAN n -D4 narrows as the percentage n of HF exchange is increased. So do sugar conformers SCONF at low HF exchange, while at SCAN0-D4 and beyond, self-consistent densities are preferred. Peptide conformers PCONF and amino acid conformers AMINO20X4 do not benefit from HF-DFT, whereas alkane conformers benefit insignificantly beyond 40%.

In contrast, for large-molecule isomerization reactions (ISOL24), one can see a benefit to HF-SCAN-D4 over SCAN-D4, and more marginally for HF-SCAN10-D4 over SCAN10-D4, but beyond that point using HF densities no longer is beneficial.

Turning now to three subsets with some static correlation effects: the W4-11 atomization energies: HF-SCAN-D4 clearly outperforms SCAN-D4, but for all hybrids considered, HF-SCAN n -D4 does more poorly than SCAN n -D4. No benefit from HF density is seen for the 13 difficult cases (DC13) subset. Here too, for the G21EA electron affinities

subset, HF-DFT does not help at all, as we observed for the other three cases (PBE n , B n LYP and TPSS n).

(c) Additional remarks:

Finally, what about range-separated hybrids? We carried out limited testing with the CAM-B3LYP⁷³ and LC-wPBE⁷⁴ range-separated hybrids. To cut a long story short: it appears that range-separated hybrids do not benefit much from HF-DFT, as so much HF exchange is already present at long range.

Double-hybrid functionals typically entail percentages of HF exchange ranging from 50% for PBE0-DH⁷⁵ and 53% for B2PLYP³⁹ to $(1/2)^{1/3} \approx 79.3\%$ for PBE0-2⁷⁶ and 81% for B2NC-PLYP⁷⁷, with the best performers situated in the range 62.2% for ω B97M(2)⁷⁸ via 65% for B2GP-PLYP⁷⁹ to 69% for revDSD-PBEP86.¹⁰ In view of the preceding, it is clear that all of these percentages are well outside the range where density-corrected DFT would be beneficial in any way.

Conclusions

From our comparative evaluation against the GMTKN55 benchmark suite of the PBE n -D4 and HF-PBE n -D4 series, as well as the corresponding series involving B n LYP, TPSS n , and SCAN n , we were able to draw the following conclusions.

- (a) For the self-consistent series, the global minimum in terms of WTMAD2 lies near $3/8$ (or 37.5%) of HF exchange, i.e., the PBE38-D4 functional proposed by Grimme;^{28,44} the loss of accuracy in small-molecule thermochemistry is compensated by gains in accuracy elsewhere, notably barrier heights. In contrast, for HF-PBE n -D4 and HF-B n LYP-D4, the global minimum lies closer to $1/4$ (25%) of HF exchange.
- (b) In general, the benefits of HF-DFT are greatest for pure GGAs and decrease monotonically with increasing HF exchange: for 50% and above, self-consistent functionals are actually superior to HF-DFT, meaning HF-DFT does not represent a general route to improve double hybrids. Likewise, HF-DFT does not offer a route for further improvement in range-separated hybrids.
- (c) With moderate HF exchange (e.g., HF-PBE0-D4, HF-B1LYP-D4), the benefits of HF-DFT are greatest in noncovalent interactions that, from a SAPT (symmetry-adapted perturbation theory) perspective, have a strong electrostatic component—such as hydrogen bonds, halogen bonds, pnictogen bonds, and the like. These

benefits are also seen in conformers and isomer equilibria that are primarily driven by intramolecular hydrogen bonding (and the like). London dispersion-dominated problems like rare-gas clusters and alkane dimers do not benefit, while HF-DFT does more harm than good for π -stacking.

- (d) In situations with significant static correlation (particularly type A), where a single HF determinant is a poor zero-order representation of the wave function, HF-DFT inherits that problem and is actually detrimental.
- (e) HF-SCAN-D4 appears to be a particularly felicitous combination, with a WTMAD2 for a nonempirical functional that compares favorably with hybrid GGAs and meta-GGAs except for the heavily parametrized M06-2X⁸⁰, and a cost that is marginally greater than a simple HF calculation.

Acknowledgments

The authors would like to thank Drs. Irena Efremenko and Mark A. Iron for helpful discussions, and Dr. Mark Vilensky (scientific computing manager of CHEMFARM) for technical assistance.

Funding Sources

This research was supported by the Israel Science Foundation (grants 1358/15 and 1969/20), and by the Minerva Foundation, Munich, Germany (grant 20/05). GS acknowledges a fellowship from the Feinberg Graduate School of the Weizmann Institute.

Supporting Information

The Supporting Information (in PDF format) is available free of charge at <https://doi.org/10.1021/xxxxxxx>.

Abridged details of all 55 subsets of GMTKN55 with proper references, optimized D4 parameters and five major subcategory contribution for total WTMAD2 for both HF and self-consistent PBE n , B n LYP, SCAN n and TPSS n functionals, figures indicating dependence of subset-wise WTMAD2 contributions on the percentage of HF exchange for the SCAN n -D4 and B n LYP-D4 series (n ranging from 0 to 50%), sample inputs for HF-DFT.

References

- (1) Wasserman, A.; Nafziger, J.; Jiang, K.; Kim, M.-C.; Sim, E.; Burke, K. The Importance of Being Inconsistent. *Annu. Rev. Phys. Chem.* **2017**, *68*, 555–581.
- (2) Bartlett, R. J. Adventures in DFT by a Wavefunction Theorist. *J. Chem. Phys.* **2019**, *151*, 160901.
- (3) Sekino, H.; Oliphant, N.; Bartlett, R. J. Property Evaluation Using the Hartree-Fock-Density-Functional-Theory Method: An Efficient Formalism for First- And Second-Order Properties. *J. Chem. Phys.* **1994**, *101*, 7788–7794.
- (4) Becke, A. D. Perspective: Fifty Years of Density-Functional Theory in Chemical Physics. *J. Chem. Phys.* **2014**, *140*, 18A301.
- (5) Lonsdale, D. R.; Goerigk, L. The One-Electron Self-Interaction Error in 74 Density Functional Approximations: A Case Study on Hydrogenic Mono- and Dinuclear Systems. *Phys. Chem. Chem. Phys.* **2020**, *22*, 15805–15830.
- (6) Kim, Y.; Song, S.; Sim, E.; Burke, K. Halogen and Chalcogen Binding Dominated by Density-Driven Errors. *J. Phys. Chem. Lett.* **2019**, *10*, 295–301.
- (7) Vuckovic, S.; Burke, K. Quantifying and Understanding Errors in Molecular Geometries. **2020**, 1–8.
- (8) Kozuch, S.; Martin, J. M. L. Halogen Bonds: Benchmarks and Theoretical Analysis. *J. Chem. Theory Comput.* **2013**, *9*, 1918–1931.
- (9) Kesharwani, M. K.; Manna, D.; Sylvetsky, N.; Martin, J. M. L. The X40×10 Halogen Bonding Benchmark Revisited: Surprising Importance of (n-1)d Subvalence Correlation. *J. Phys. Chem. A* **2018**, *122*, 2184–2197.
- (10) Santra, G.; Sylvetsky, N.; Martin, J. M. L. Minimally Empirical Double-Hybrid Functionals Trained against the GMTKN55 Database: RevDSD-PBEP86-D4, RevDOD-PBE-D4, and DOD-SCAN-D4. *J. Phys. Chem. A* **2019**, *123*, 5129–5143.
- (11) Martin, J. M. L.; Santra, G. Empirical Double-Hybrid Density Functional Theory: A ‘Third Way’ in Between WFT and DFT. *Isr. J. Chem.* **2020**, *60*, 787–804.
- (12) Goerigk, L.; Hansen, A.; Bauer, C.; Ehrlich, S.; Najibi, A.; Grimme, S. A Look at the Density Functional Theory Zoo with the Advanced GMTKN55 Database for General Main Group Thermochemistry, Kinetics and Noncovalent Interactions. *Phys. Chem.*

- Chem. Phys.* **2017**, *19*, 32184–32215.
- (13) Cioslowski, J. Density-Driven Self-Consistent-Field Method: Density-Constrained Correlation Energies in the Helium Series. *Phys. Rev. A* **1991**, *43*, 1223–1228.
- (14) Ramos-Cordoba, E.; Salvador, P.; Matito, E. Separation of Dynamic and Nondynamic Correlation. *Phys. Chem. Chem. Phys.* **2016**, *18*, 24015–24023.
- (15) Huber, P. J.; Ronchetti, E. M. *Robust Statistics*; Wiley Series in Probability and Statistics; John Wiley & Sons, Inc.: Hoboken, NJ, USA, 2009.
- (16) Geary, R. C. The Ratio of the Mean Deviation to the Standard Deviation as a Test of Normality. *Biometrika* **1935**, *27*, 310–332.
- (17) Frisch, M. J.; Trucks, G. W.; Schlegel, H. B.; Scuseria, G. E.; Robb, M. A.; Cheeseman, J. R.; Scalmani, G.; Barone, V.; Petersson, G. A.; Nakatsuji, H.; Li, X.; Caricato, M.; Marenich, A. V.; Bloino, J.; Janesko, B. G.; Gomperts, R.; Mennucci, B.; Hratchian, H. P.; Ortiz, J. V.; Izmaylov, A. F.; Sonnenberg, J. L.; Williams-Young, D.; Ding, F.; Lipparini, F.; Egidi, F.; Goings, J.; Peng, B.; Petrone, A.; Henderson, T.; Ranasinghe, D.; Zakrzewski, V. G.; Gao, J.; Rega, N.; Zheng, G.; Liang, W.; Hada, M.; Ehara, M.; Toyota, K.; Fukuda, R.; Hasegawa, J.; Ishida, M.; Nakajima, T.; Honda, Y.; Kitao, O.; Nakai, H.; Vreven, T.; Throssell, K.; Montgomery Jr., J. A.; Peralta, J. E.; Ogliaro, F.; Bearpark, M. J.; Heyd, J. J.; Brothers, E. N.; Kudin, K. N.; Staroverov, V. N.; Keith, T. A.; Kobayashi, R.; Normand, J.; Raghavachari, K.; Rendell, A. P.; Burant, J. C.; Iyengar, S. S.; Tomasi, J.; Cossi, M.; Millam, J. M.; Klene, M.; Adamo, C.; Cammi, R.; Ochterski, J. W.; Martin, R. L.; Morokuma, K.; Farkas, O.; Foresman, J. B.; Fox, D. J. *Gaussian 16 Revision C.01*; Gaussian, Inc.: Wallingford, CT, 2016.
- (18) Neese, F.; Wennmohs, F.; Becker, U.; Riplinger, C. The ORCA Quantum Chemistry Program Package. *J. Chem. Phys.* **2020**, *152*, 224108.
- (19) Shao, Y.; Gan, Z.; Epifanovsky, E.; Gilbert, A. T. B.; Wormit, M.; Kussmann, J.; Lange, A. W.; Behn, A.; Deng, J.; Feng, X.; Ghosh, D.; Goldey, M.; Horn, P. R.; Jacobson, L. D.; Kaliman, I.; Khaliullin, R. Z.; Kuś, T.; Landau, A.; Liu, J.; Proynov, E. I.; Rhee, Y. M.; Richard, R. M.; Rohrdanz, M. a.; Steele, R. P.; Sundstrom, E. J.; Woodcock, H. L.; Zimmerman, P. M.; Zuev, D.; Albrecht, B.; Alguire, E.; Austin, B.; Beran, G. J. O.; Bernard, Y. a.; Berquist, E.; Brandhorst, K.; Bravaya, K. B.; Brown, S.

- T.; Casanova, D.; Chang, C.-M.; Chen, Y.; Chien, S. H.; Closser, K. D.; Crittenden, D. L.; Diedenhofen, M.; DiStasio, R. A.; Do, H.; Dutoi, A. D.; Edgar, R. G.; Fatehi, S.; Fusti-Molnar, L.; Ghysels, A.; Golubeva-Zadorozhnaya, A.; Gomes, J.; Hanson-Heine, M. W. D.; Harbach, P. H. P.; Hauser, A. W.; Hohenstein, E. G.; Holden, Z. C.; Jagau, T.-C.; Ji, H.; Kaduk, B.; Khistyayev, K.; Kim, J.; Kim, J.; King, R. a.; Klunzinger, P.; Kosenkov, D.; Kowalczyk, T.; Krauter, C. M.; Lao, K. U.; Laurent, A. D.; Lawler, K. V.; Levchenko, S. V.; Lin, C. Y.; Liu, F.; Livshits, E.; Lochan, R. C.; Luenser, A.; Manohar, P.; Manzer, S. F.; Mao, S.-P.; Mardirossian, N.; Marenich, A. V.; Maurer, S. a.; Mayhall, N. J.; Neuscamman, E.; Oana, C. M.; Olivares-Amaya, R.; O'Neill, D. P.; Parkhill, J. a.; Perrine, T. M.; Peverati, R.; Prociuk, A.; Rehn, D. R.; Rosta, E.; Russ, N. J.; Sharada, S. M.; Sharma, S.; Small, D. W.; Sodt, A.; Stein, T.; Stück, D.; Su, Y.-C.; Thom, A. J. W.; Tsuchimochi, T.; Vanovschi, V.; Vogt, L.; Vydrov, O.; Wang, T.; Watson, M. a.; Wenzel, J.; White, A.; Williams, C. F.; Yang, J.; Yeganeh, S.; Yost, S. R.; You, Z.-Q.; Zhang, I. Y.; Zhang, X.; Zhao, Y.; Brooks, B. R.; Chan, G. K. L.; Chipman, D. M.; Cramer, C. J.; Goddard, W. A.; Gordon, M. S.; Hehre, W. J.; Klamt, A.; Schaefer, H. F.; Schmidt, M. W.; Sherrill, C. D.; Truhlar, D. G.; Warshel, A.; Xu, X.; Aspuru-Guzik, A.; Baer, R.; Bell, A. T.; Besley, N. a.; Chai, J.-D.; Dreuw, A.; Dunietz, B. D.; Furlani, T. R.; Gwaltney, S. R.; Hsu, C.-P.; Jung, Y.; Kong, J.; Lambrecht, D. S.; Liang, W.; Ochsenfeld, C.; Rassolov, V. a.; Slipchenko, L. V.; Subotnik, J. E.; Van Voorhis, T.; Herbert, J. M.; Krylov, A. I.; Gill, P. M. W.; Head-Gordon, M. Advances in Molecular Quantum Chemistry Contained in the Q-Chem 4 Program Package. *Mol. Phys.* **2015**, *113*, 184–215.
- (20) Weigend, F.; Ahlrichs, R. Balanced Basis Sets of Split Valence, Triple Zeta Valence and Quadruple Zeta Valence Quality for H to Rn: Design and Assessment of Accuracy. *Phys. Chem. Chem. Phys.* **2005**, *7*, 3297–3305.
- (21) Rappoport, D.; Furche, F. Property-Optimized Gaussian Basis Sets for Molecular Response Calculations. *J. Chem. Phys.* **2010**, *133*, 134105.
- (22) Weigend, F. A Fully Direct RI-HF Algorithm: Implementation, Optimised Auxiliary Basis Sets, Demonstration of Accuracy and Efficiency. *Phys. Chem. Chem. Phys.* **2002**, *4*, 4285–4291.
- (23) Sun, J.; Ruzsinszky, A.; Perdew, J. P. Strongly Constrained and Appropriately Normed Semilocal Density Functional. *Phys. Rev. Lett.* **2015**, *115*, 036402.

- (24) Brandenburg, J. G.; Bates, J. E.; Sun, J.; Perdew, J. P. Benchmark Tests of a Strongly Constrained Semilocal Functional with a Long-Range Dispersion Correction. *Phys. Rev. B - Condens. Matter Mater. Phys.* **2016**, *94*, 17–19.
- (25) Dasgupta, S.; Herbert, J. M. Standard Grids for High-Precision Integration of Modern Density Functionals: SG-2 and SG-3. *J. Comput. Chem.* **2017**, *38*, 869–882.
- (26) Perdew, J. P.; Burke, K.; Ernzerhof, M. Generalized Gradient Approximation Made Simple. *Phys. Rev. Lett.* **1996**, *77*, 3865–3868.
- (27) Burke, K.; Ernzerhof, M.; Perdew, J. P. The Adiabatic Connection Method: A Non-Empirical Hybrid. *Chem. Phys. Lett.* **1997**, *265*, 115–120.
- (28) Grimme, S.; Antony, J.; Ehrlich, S.; Krieg, H. A Consistent and Accurate Ab Initio Parametrization of Density Functional Dispersion Correction (DFT-D) for the 94 Elements H-Pu. *J. Chem. Phys.* **2010**, *132*, 154104.
- (29) Bernard, Y. A.; Shao, Y.; Krylov, A. I. General Formulation of Spin-Flip Time-Dependent Density Functional Theory Using Non-Collinear Kernels: Theory, Implementation, and Benchmarks. *J. Chem. Phys.* **2012**, *136*, 204103.
- (30) Baer, R.; Neuhauser, D. Density Functional Theory with Correct Long-Range Asymptotic Behavior. *Phys. Rev. Lett.* **2005**, *94*, 2–5.
- (31) Lee, C.; Yang, W.; Parr, R. G. Development of the Colle-Salvetti Correlation-Energy Formula into a Functional of the Electron Density. *Phys. Rev. B* **1988**, *37*, 785–789.
- (32) Stephens, P. J.; Devlin, F. J.; Chabalowski, C. F.; Frisch, M. J. Ab Initio Calculation of Vibrational Absorption and Circular Dichroism Spectra Using Density Functional Force Fields. *J. Phys. Chem.* **1994**, *98*, 11623–11627.
- (33) Adamo, C.; Barone, V. Toward Reliable Adiabatic Connection Models Free from Adjustable Parameters. *Chem. Phys. Lett.* **1997**, *274*, 242–250.
- (34) Becke, A. D. A New Mixing of Hartree–Fock and Local Density-functional Theories. *J. Chem. Phys.* **1993**, *98*, 1372–1377.
- (35) Tao, J.; Perdew, J.; Staroverov, V.; Scuseria, G. Climbing the Density Functional Ladder: Nonempirical Meta–Generalized Gradient Approximation Designed for Molecules and Solids. *Phys. Rev. Lett.* **2003**, *91*, 146401.

- (36) Perdew, J. P.; Tao, J.; Staroverov, V. N.; Scuseria, G. E. Meta-Generalized Gradient Approximation: Explanation of a Realistic Nonempirical Density Functional. *J. Chem. Phys.* **2004**, *120*, 6898–6911.
- (37) Caldeweyher, E. J. Development and Application of London Dispersion Corrections for Electronic Structure Methods (Ph.D. Thesis), U. Bonn, Germany, 2020.
- (38) Caldeweyher, E.; Ehlert, S.; Hansen, A.; Neugebauer, H.; Spicher, S.; Bannwarth, C.; Grimme, S. A Generally Applicable Atomic-Charge Dependent London Dispersion Correction. *J. Chem. Phys.* **2019**, *150*, 154122.
- (39) Grimme, S. Semiempirical Hybrid Density Functional with Perturbative Second-Order Correlation. *J. Chem. Phys.* **2006**, *124*, 034108.
- (40) Axilrod, B. M.; Teller, E. Interaction of the van Der Waals Type Between Three Atoms. *J. Chem. Phys.* **1943**, *11*, 299–300.
- (41) Muto, Y. Force between Nonpolar Molecules. *Proc. Physico-Mathematical Soc. Japan* **1943**, *17*, 629–631.
- (42) Powell, M. The BOBYQA Algorithm for Bound Constrained Optimization without Derivatives (DAMPT Report 2009/NA06); Department of Applied Mathematics and Theoretical Physics, University of Cambridge, UK, 2009.
- (43) Adamo, C.; Barone, V. Toward Reliable Density Functional Methods without Adjustable Parameters: The PBE0 Model. *J. Chem. Phys.* **1999**, *110*, 6158–6170.
- (44) Goerigk, L.; Grimme, S. A Thorough Benchmark of Density Functional Methods for General Main Group Thermochemistry, Kinetics, and Noncovalent Interactions. *Phys. Chem. Chem. Phys.* **2011**, *13*, 6670–6688.
- (45) Durant, J. L. Evaluation of Transition State Properties by Density Functional Theory. *Chem. Phys. Lett.* **1996**, *256*, 595–602.
- (46) Lynch, B. J.; Fast, P. L.; Harris, M.; Truhlar, D. G. Adiabatic Connection for Kinetics. *J. Phys. Chem. A* **2000**, *104*, 4813–4815.
- (47) Boese, A. D.; Martin, J. M. L. Development of Density Functionals for Thermochemical Kinetics. *J. Chem. Phys.* **2004**, *121*, 3405–3416.
- (48) Zhao, Y.; Truhlar, D. G. Exploring the Limit of Accuracy of the Global Hybrid Meta

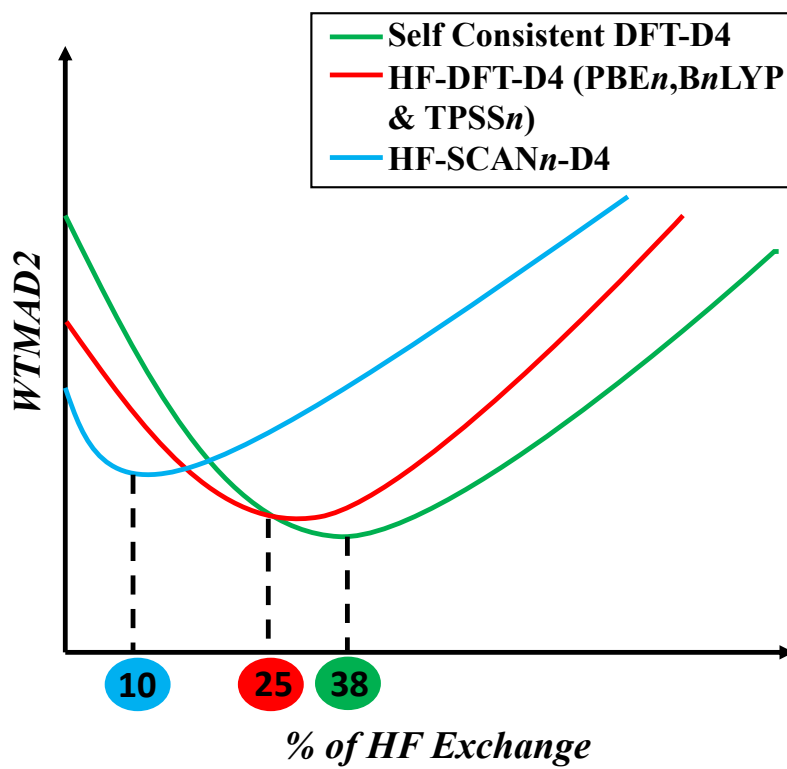
- Density Functional for Main-Group Thermochemistry, Kinetics, and Noncovalent Interactions. *J. Chem. Theory Comput.* **2008**, *4*, 1849–1868.
- (49) Zhang, Y.; Yang, W. A Challenge for Density Functionals: Self-Interaction Error Increases for Systems with a Noninteger Number of Electrons. *J. Chem. Phys.* **1998**, *109*, 2604–2608.
- (50) Tsuneda, T.; Kamiya, M.; Hirao, K. Regional Self-Interaction Correction of Density Functional Theory. *J. Comput. Chem.* **2003**, *24*, 1592–1598.
- (51) Zope, R. R.; Yamamoto, Y.; Diaz, C. M.; Baruah, T.; Peralta, J. E.; Jackson, K. A.; Santra, B.; Perdew, J. P. A Step in the Direction of Resolving the Paradox of Perdew-Zunger Self-Interaction Correction. *J. Chem. Phys.* **2019**, *151*, 214108.
- (52) Li, L.; Trepte, K.; Jackson, K. A.; Johnson, J. K. Application of Self-Interaction Corrected Density Functional Theory to Early, Middle, and Late Transition States. *J. Phys. Chem. A* **2020**.
- (53) Janesko, B. G.; Scuseria, G. E. Hartree-Fock Orbitals Significantly Improve the Reaction Barrier Heights Predicted by Semilocal Density Functionals. *J. Chem. Phys.* **2008**, *128*, 244112.
- (54) Mahler, A.; Janesko, B. G.; Moncho, S.; Brothers, E. N. Why Are GGAs so Accurate for Reaction Kinetics on Surfaces? Systematic Comparison of Hybrid vs. Nonhybrid DFT for Representative Reactions. *J. Chem. Phys.* **2017**, *146*.
- (55) Mahler, A.; Janesko, B. G.; Moncho, S.; Brothers, E. N. When Hartree-Fock Exchange Admixture Lowers DFT-Predicted Barrier Heights: Natural Bond Orbital Analyses and Implications for Catalysis. *J. Chem. Phys.* **2018**, *148*, 244106.
- (56) Grimme, S. Semiempirical GGA-Type Density Functional Constructed with a Long-Range Dispersion Correction. *J. Comput. Chem.* **2006**, *27*, 1787–1799.
- (57) Zhao, Y.; González-García, N.; Truhlar, D. G. Benchmark Database of Barrier Heights for Heavy Atom Transfer, Nucleophilic Substitution, Association, and Unimolecular Reactions and Its Use to Test Theoretical Methods. *J. Phys. Chem. A* **2005**, *109*, 2012–2018.
- (58) Zhao, Y.; Lynch, B. J.; Truhlar, D. G. Multi-Coefficient Extrapolated Density Functional Theory for Thermochemistry and Thermochemical Kinetics. *Phys. Chem.*

- Chem. Phys.* **2005**, *7*, 43.
- (59) Karton, A.; Goerigk, L. Accurate Reaction Barrier Heights of Pericyclic Reactions: Surprisingly Large Deviations for the CBS-QB3 Composite Method and Their Consequences in DFT Benchmark Studies. *J. Comput. Chem.* **2015**, *36*, 622–632.
- (60) Szalewicz, K. Symmetry-Adapted Perturbation Theory of Intermolecular Forces. *Wiley Interdiscip. Rev. Comput. Mol. Sci.* **2012**, *2*, 254–272.
- (61) Rezáč, J.; Riley, K. E.; Hobza, P. S66: A Well-Balanced Database of Benchmark Interaction Energies Relevant to Biomolecular Structures. *J. Chem. Theory Comput.* **2011**, *7*, 2427–2438.
- (62) Kesharwani, M. K.; Karton, A.; Sylvetsky, N.; Martin, J. M. L. The S66 Non-Covalent Interactions Benchmark Reconsidered Using Explicitly Correlated Methods Near the Basis Set Limit. *Aust. J. Chem.* **2018**, *71*, 238.
- (63) Kozuch, S.; Bachrach, S. M.; Martin, J. M. L. Conformational Equilibria in Butane-1,4-Diol: A Benchmark of a Prototypical System with Strong Intramolecular H-Bonds. *J. Phys. Chem. A* **2014**, *118*, 293–303.
- (64) Kesharwani, M. K.; Karton, A.; Martin, J. M. L. Benchmark Ab Initio Conformational Energies for the Proteinogenic Amino Acids through Explicitly Correlated Methods. Assessment of Density Functional Methods. *J. Chem. Theory Comput.* **2016**, *12*, 444–454.
- (65) Yuan, Y.; Mills, M. J. L.; Popelier, P. L. A.; Jensen, F. Comprehensive Analysis of Energy Minima of the 20 Natural Amino Acids. *J. Phys. Chem. A* **2014**, *118*, 7876–7891.
- (66) Tschumper, G. S.; Schaefer, H. F. Predicting Electron Affinities with Density Functional Theory: Some Positive Results for Negative Ions. *J. Chem. Phys.* **1997**, *107*, 2529–2541.
- (67) de Oliveira, G.; Martin, J. M. L.; de Proft, F.; Geerlings, P. Electron Affinities of the First- and Second-Row Atoms: Benchmark Ab Initio and Density-Functional Calculations. *Phys. Rev. A* **1999**, *60*, 1034–1045.
- (68) Karton, A.; Daon, S.; Martin, J. M. L. W4-11: A High-Confidence Benchmark Dataset for Computational Thermochemistry Derived from First-Principles W4 Data. *Chem.*

- Phys. Lett.* **2011**, *510*, 165–178.
- (69) Santra, G.; Martin, J. M. L. Some Observations on the Performance of the Most Recent Exchange-Correlation Functionals for the Large and Chemically Diverse GMTKN55 Benchmark. *AIP Conf. Proc.* **2019**, *2186*, 030004.
- (70) Najibi, A.; Goerigk, L. The Nonlocal Kernel in van Der Waals Density Functionals as an Additive Correction: An Extensive Analysis with Special Emphasis on the B97M-V and ω B97M-V Approaches. *J. Chem. Theory Comput.* **2018**, *14*, 5725–5738.
- (71) Mardirossian, N.; Head-Gordon, M. ω B97X-V: A 10-Parameter, Range-Separated Hybrid, Generalized Gradient Approximation Density Functional with Nonlocal Correlation, Designed by a Survival-of-the-Fittest Strategy. *Phys. Chem. Chem. Phys.* **2014**, *16*, 9904–9924.
- (72) Mardirossian, N.; Head-Gordon, M. ω B97M-V: A Combinatorially Optimized, Range-Separated Hybrid, Meta-GGA Density Functional with VV10 Nonlocal Correlation. *J. Chem. Phys.* **2016**, *144*, 214110.
- (73) Yanai, T.; Tew, D. P.; Handy, N. C. A New Hybrid Exchange–Correlation Functional Using the Coulomb-Attenuating Method (CAM-B3LYP). *Chem. Phys. Lett.* **2004**, *393*, 51–57.
- (74) Vydrov, O. a; Scuseria, G. E. Assessment of a Long-Range Corrected Hybrid Functional. *J. Chem. Phys.* **2006**, *125*, 234109.
- (75) Brémond, E.; Adamo, C. Seeking for Parameter-Free Double-Hybrid Functionals: The PBE0-DH Model. *J. Chem. Phys.* **2011**, *135*, 024106.
- (76) Chai, J. Da; Mao, S. P. Seeking for Reliable Double-Hybrid Density Functionals without Fitting Parameters: The PBE0-2 Functional. *Chem. Phys. Lett.* **2012**, *538*, 121–125.
- (77) Yu, F. Double-Hybrid Density Functionals Free of Dispersion and Counterpoise Corrections for Non-Covalent Interactions. *J. Phys. Chem. A* **2014**, *118*, 3175–3182.
- (78) Mardirossian, N.; Head-Gordon, M. Survival of the Most Transferable at the Top of Jacob’s Ladder: Defining and Testing the ω B97M(2) Double Hybrid Density Functional. *J. Chem. Phys.* **2018**, *148*, 241736.
- (79) Karton, A.; Tarnopolsky, A.; Lamère, J.-F.; Schatz, G. C.; Martin, J. M. L. Highly

- Accurate First-Principles Benchmark Data Sets for the Parametrization and Validation of Density Functional and Other Approximate Methods. Derivation of a Robust, Generally Applicable, Double-Hybrid Functional for Thermochemistry and Thermochemical . *J. Phys. Chem. A* **2008**, *112*, 12868–12886.
- (80) Zhao, Y.; Truhlar, D. G. The M06 Suite of Density Functionals for Main Group Thermochemistry, Thermochemical Kinetics, Noncovalent Interactions, Excited States, and Transition Elements: Two New Functionals and Systematic Testing of Four M06-Class Functionals and 12 Other Function. *Theor. Chem. Acc.* **2008**, *120*, 215–241.
- (81) Becke, A. D. Density-Functional Exchange-Energy Approximation with Correct Asymptotic Behavior. *Phys. Rev. A* **1988**, *38*, 3098–3100.
- (82) Vosko, S. H.; Wilk, L.; Nusair, M. Accurate Spin-Dependent Electron Liquid Correlation Energies for Local Spin Density Calculations: A Critical Analysis. *Can. J. Phys.* **1980**, *58*, 1200–1211.

TABLE OF CONTENTS GRAPHIC



Electronic Supporting Information

What types of chemical problems benefit from density-corrected DFT? A probe using an extensive and chemically diverse test suite

*Golokesh Santra and Jan M.L. Martin**

Department of Organic Chemistry, Weizmann Institute of Science, 7610001 Rehovot, Israel.

Email: gershom@weizmann.ac.il

Table S1: Abbreviations used and their descriptions

Abbreviation	Description
ACONF ¹	Relative energies of alkane conformers
ADIM6 ²	Interaction energies of n-alkane dimers
AHB21 ³	Interaction energies in anion–neutral dimers
AL2X6 ⁴	Dimerisation energies of AlX ₃ compounds
ALK8 ⁴	Dissociation and other reactions of alkaline compounds
ALKBDE10 ⁵	Dissociation energies in group-1 and -2 diatomics
AMINO20X4 ⁶	Relative energies in amino acid conformers
BH76RC ⁷	Barrier heights of hydrogen transfer, heavy atom transfer, nucleophilic substitution, unimolecular and association reactions
BH76 ^{8,9,7}	Reaction energies of the BH7610,11,23 set
BHDIV10 ⁴	Diverse reaction barrier heights
BHPERI ^{4,10,11,12}	Barrier heights of pericyclic reactions
BHROT27 ⁴	Barrier heights for rotation around single bonds
BSR36 ^{13,14}	Bond-separation reactions of saturated hydrocarbons
BUT14DIOL ¹⁵	Relative energies in butane-1,4-diol conformers
C60ISO ¹⁶	Relative energies between C60 isomers
CARBHB12 ⁴	Hydrogen-bonded complexes between carbene analogues and H ₂ O, NH ₃ , or HCl
CDIE20 ¹⁷	Double-bond isomerisation energies in cyclic systems
CHB6 ³	Interaction energies in cation–neutral dimers
DARC ^{7,18}	Reaction energies of Diels–Alder reactions
DC13 ^{19,7,20,21–29}	13 difficult cases for DFT methods
DIPCS10 ⁴	Double-ionisation potentials of closed-shell systems
FH51 ^{30,31}	Reaction energies in various (in-)organic systems
G21EA ^{7,32}	Adiabatic electron affinities
G21IP ^{7,32}	Adiabatic ionisation potentials
G2RC ^{7,33}	Reaction energies of selected G2/97 systems
HAL59 ^{34,35}	Binding energies in halogenated dimers (incl. halogen bonds)
HEAVY28 ⁹	Noncovalent interaction energies between heavy element hydrides
HEAVYSB11 ⁴	Dissociation energies in heavy-element compounds
ICONF ⁴	Relative energies in conformers of inorganic systems
IDISP ^{7,36–39}	Intramolecular dispersion interactions
IL16 ³	Interaction energies in anion–cation dimers
INV24 ⁴⁰	Inversion/racemisation barrier heights
ISO34 ³⁶	Isomerisation energies of small and medium-sized organic molecules
ISOL24 ⁴¹	Isomerisation energies of large organic molecules
MB16-43 ⁴	Decomposition energies of artificial molecules
MCONF ⁴²	Relative energies in melatonin conformers
NBPRC ^{7,38,43}	Oligomerisations and H ₂ fragmentations of NH ₃ /BH ₃ systems; H ₂ activation reactions with PH ₃ /BH ₃ systems
PA26 ⁴	Adiabatic proton affinities (incl. of amino acids)
PArel ⁴	Relative energies in protonated isomers
PCONF21	Relative energies in tri- and tetrapeptide conformers
PNICO23 ⁴⁴	Interaction energies in pnictogen-containing dimers
PX13 ⁴⁵	Proton-exchange barriers in H ₂ O, NH ₃ , and HF clusters
RC21 ⁴	Fragmentations and rearrangements in radical cations
RG18 ⁴	Interaction energies in rare-gas complexes
RSE43 ⁴⁶	Radical-stabilisation energies
S22 ⁴⁷	Binding energies of noncovalently bound dimers

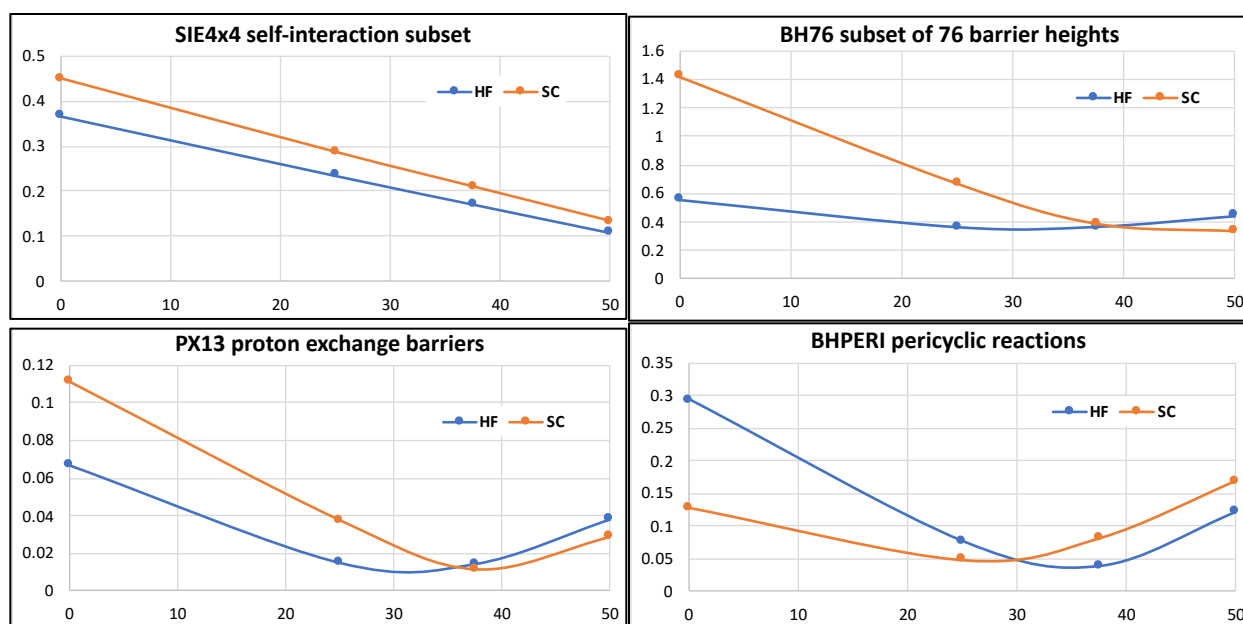
S66 ⁴⁸	Binding energies of noncovalently bound dimers
SCONF ^{7,49}	Relative energies of sugar conformers
SIE4X4 ⁵⁰	Self-interaction-error related problems
TAUT15 ⁴	Relative energies in tautomers
UPU23 ⁵¹	Relative energies between RNA-backbone conformers
W4-11 ⁵²	Total atomisation energies
WATER27 ⁵³	Binding energies in (H ₂ O) _n , H+(H ₂ O) _n and OH-(H ₂ O) _n
WCPT18 ⁵⁴	Proton-transfer barriers in uncatalysed and water-catalysed reactions
YBDE18 ⁵⁵	Bond-dissociation energies in ylides

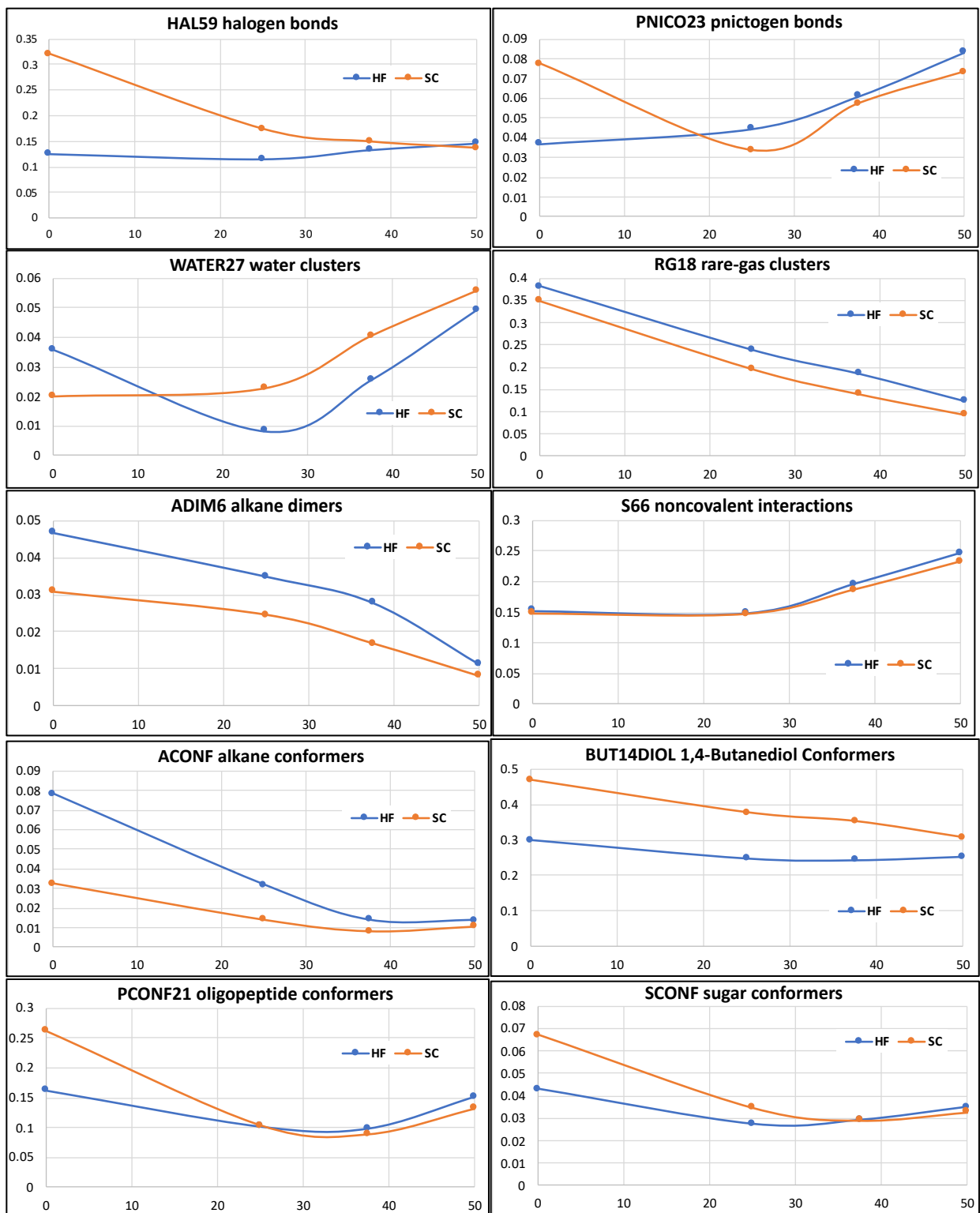
Table S2: Original and Optimized D4 parameters for HF-DFT and self-consistent DFT functionals together with five major subcategories of total WTMD2

Functionals	S ₆	a ₁	S ₈	a ₂	THERMO	BARRIER	LARGE	CONFOR	INTERMOL	WTMD2
HF-PBE-D4	1.0	0.5586	1.1145	3.6542	1.473	1.372	1.454	1.074	0.900	6.273
HF-PBE0-D4	1.0	0.4909	1.0402	4.2328	1.232	0.843	1.227	0.927	0.786	5.014
HF-PBE38-D4	1.0	0.4560	1.0815	4.5749	1.483	0.758	1.315	0.959	0.838	5.353
HF-PBE50-D4	1.0	0.4042	0.7455	4.7098	1.717	0.831	1.486	0.997	0.985	6.016
HF-BLYP-D4	1.0	0.4826	1.7143	3.2824	1.528	1.121	1.569	1.225	1.110	6.553
HF-B3LYP-D4	1.0	0.4196	1.2556	3.7554	1.146	0.675	1.208	0.949	0.827	4.804
HF-B1LYP-D4	1.0	0.4102	1.1892	3.7353	1.279	0.600	1.188	0.939	0.835	4.840
HF-B38LYP-D4	1.0	0.3754	0.8643	3.8684	1.368	0.613	1.078	0.893	0.907	4.860
HF-BHLYP-D4	1.0	0.3624	0.6822	3.9886	1.563	0.879	1.069	0.988	1.000	5.499
HF-TPSS-D4	1.0	0.3303	1.3673	4.5177	1.424	0.891	1.566	0.853	0.975	5.709
HF-TPSSh-D4	1.0	0.5162	1.4287	3.7716	1.375	1.015	1.362	0.841	0.848	5.441
HF-TPSS0-D4	1.0	0.4743	1.2502	4.0521	1.449	0.817	1.214	0.755	0.859	5.094
HF-TPSS38-D4	1.0	0.4198	0.7804	4.1058	1.605	0.811	1.260	0.767	0.938	5.381
HF-TPSS50-D4	1.0	0.3928	0.7222	4.3802	1.894	0.932	1.387	0.885	1.027	6.125
HF-SCAN-D4	1.0	0.1586	0.7155	7.4456	1.303	1.045	1.075	0.900	0.757	5.079
HF-SCAN10-D4	1.0	0.2161	1.0159	7.3021	1.334	0.898	1.059	0.905	0.764	4.960
HF-SCAN0-D4	1.0	0.2290	1.0482	7.2144	1.509	0.786	1.141	0.949	0.787	5.172
HF-SCAN38-D4	1.0	0.2493	0.8788	6.9488	1.702	0.767	1.254	1.008	0.849	5.579
HF-SCAN50-D4	1.0	0.2810	0.5959	6.4527	1.947	0.849	1.374	1.067	0.943	6.181
PBE-D4	1.0	0.7233	4.7411	4.7199	2.052	2.319	2.114	1.812	1.618	9.914
PBE-D4 ^{orig} ¹	1.0	0.3857	0.9595	4.8069	2.078	2.407	1.946	1.879	2.117	10.426
PBE0-D4	1.0	0.5835	4.3194	5.3549	1.336	1.144	1.412	1.245	1.065	6.202
PBE0-D4 ^{orig} ¹	1.0	0.4009	1.2007	5.0293	1.361	1.204	1.342	1.245	1.267	6.418
PBE38-D4	1.0	0.5208	2.8361	5.2438	1.482	0.762	1.331	1.098	0.981	5.653
PBE50-D4	1.0	0.4424	1.9249	5.3064	1.714	0.641	1.395	1.074	1.024	5.848
BLYP-D4	1.0	0.4702	3.6496	4.6263	2.062	1.931	2.461	1.629	1.282	9.365

¹ All “original” parameters are taken from ref^{56,57}.

BLYP-D4orig ¹	1.0	0.4449	2.3408	4.0933	2.006	2.066	2.188	1.851	1.493	9.603
B3LYP-D4	1.0	0.4635	2.5224	4.5658	1.327	1.099	1.722	1.202	0.911	6.261
B3LYP-D4orig ¹	1.0	0.4087	2.0293	4.5381	1.301	1.124	1.610	1.235	1.096	6.366
B1LYP-D4	1.0	0.4296	1.8888	4.3733	1.376	0.900	1.548	1.045	0.849	5.717
B1LYP-D4orig ¹	1.0	0.3931	1.9855	4.5547	1.360	0.898	1.505	1.083	0.949	5.794
B38LYP-D4	1.0	0.3999	1.2738	4.2818	1.405	0.660	1.202	0.950	0.873	5.090
BHLYP-D4	1.0	0.3665	0.9499	4.4188	1.579	0.791	1.073	1.005	0.926	5.374
BHLYP-D4orig ¹	1.0	0.2726	1.6528	5.4863	1.601	0.839	1.192	1.074	0.940	5.646
TPSS-D4	1.0	0.5886	5.4374	5.0607	1.912	2.064	2.111	1.524	1.265	8.876
TPSS-D4orig ¹	1.0	0.4282	1.7660	4.5426	1.819	2.177	1.862	1.726	1.629	9.213
TPSSh-D4	1.0	0.5634	4.4400	4.9713	2.068	1.616	1.748	1.267	1.110	7.809
TPSSh-D4orig ¹	1.0	0.4429	1.8590	4.6023	1.577	1.694	1.593	1.391	1.307	7.562
TPSS0-D4	1.0	0.5050	3.3687	5.0625	1.496	1.045	1.340	0.992	0.969	5.842
TPSS0-D4orig ¹	1.0	0.4033	1.6244	4.8054	1.504	1.103	1.246	1.054	1.102	6.008
TPSS38-D4	1.0	0.4652	2.6661	5.1069	1.613	0.764	1.244	0.916	0.939	5.477
TPSS50-D4	1.0	0.4144	1.6981	5.0215	1.858	0.808	1.304	0.917	1.001	5.887
SCAN-D4	1.0	0.1898	3.0789	9.0102	2.330	1.895	1.360	1.226	1.594	8.404
SCAN-D4orig ¹	1.0	0.6293	1.4613	6.3128	2.331	1.898	1.347	1.237	1.708	8.521
SCAN10-D4	1.0	0.3149	6.4925	8.7697	1.531	1.510	1.228	1.105	1.419	6.793
SCAN0-D4	1.0	0.3750	6.1187	8.1124	1.549	1.040	1.192	1.001	1.198	5.980
SCAN38-D4	1.0	0.3996	5.0438	7.6249	1.691	0.768	1.256	0.997	1.075	5.788
SCAN50-D4	1.0	0.4108	3.2856	6.9783	1.901	0.754	1.377	1.055	1.051	6.138





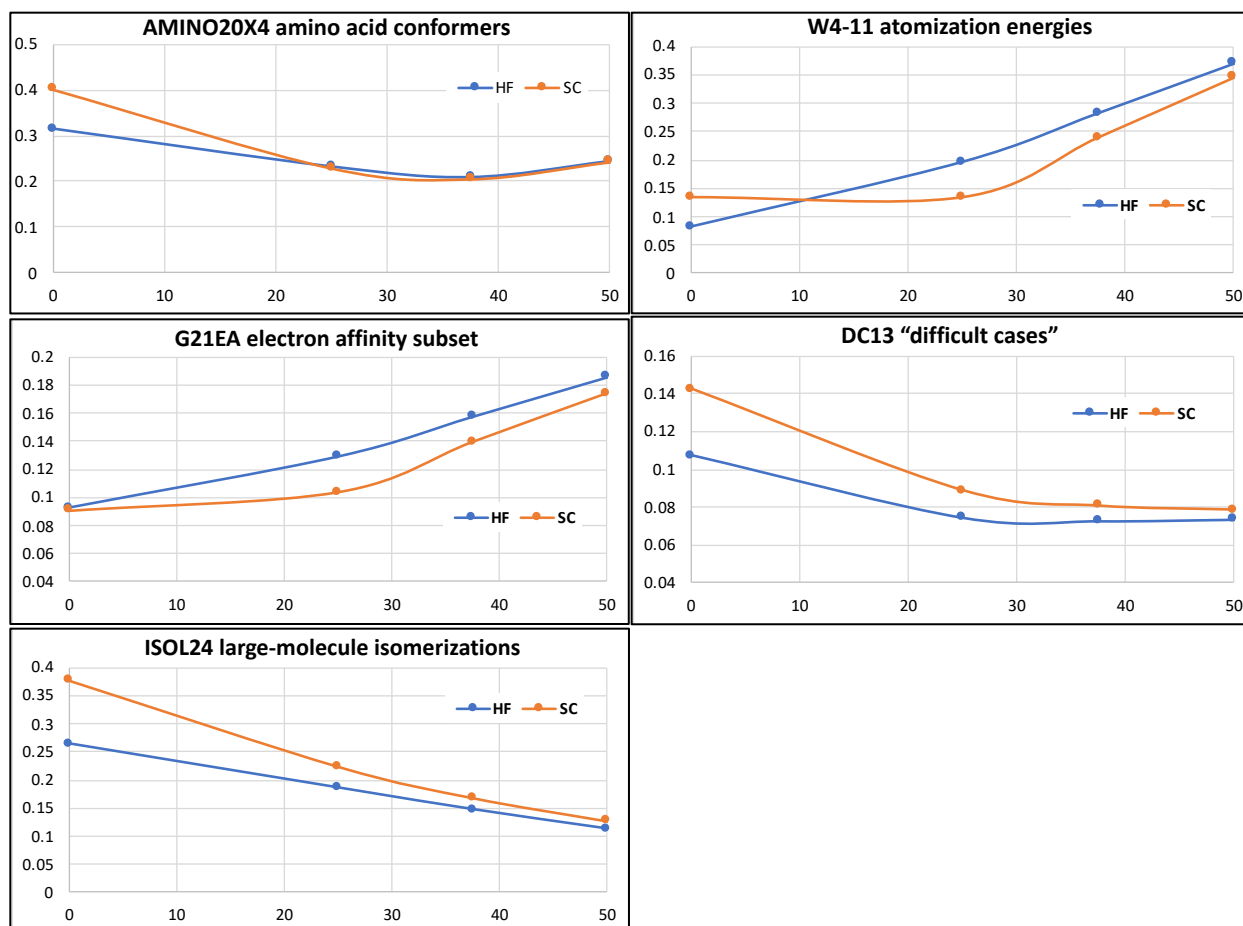
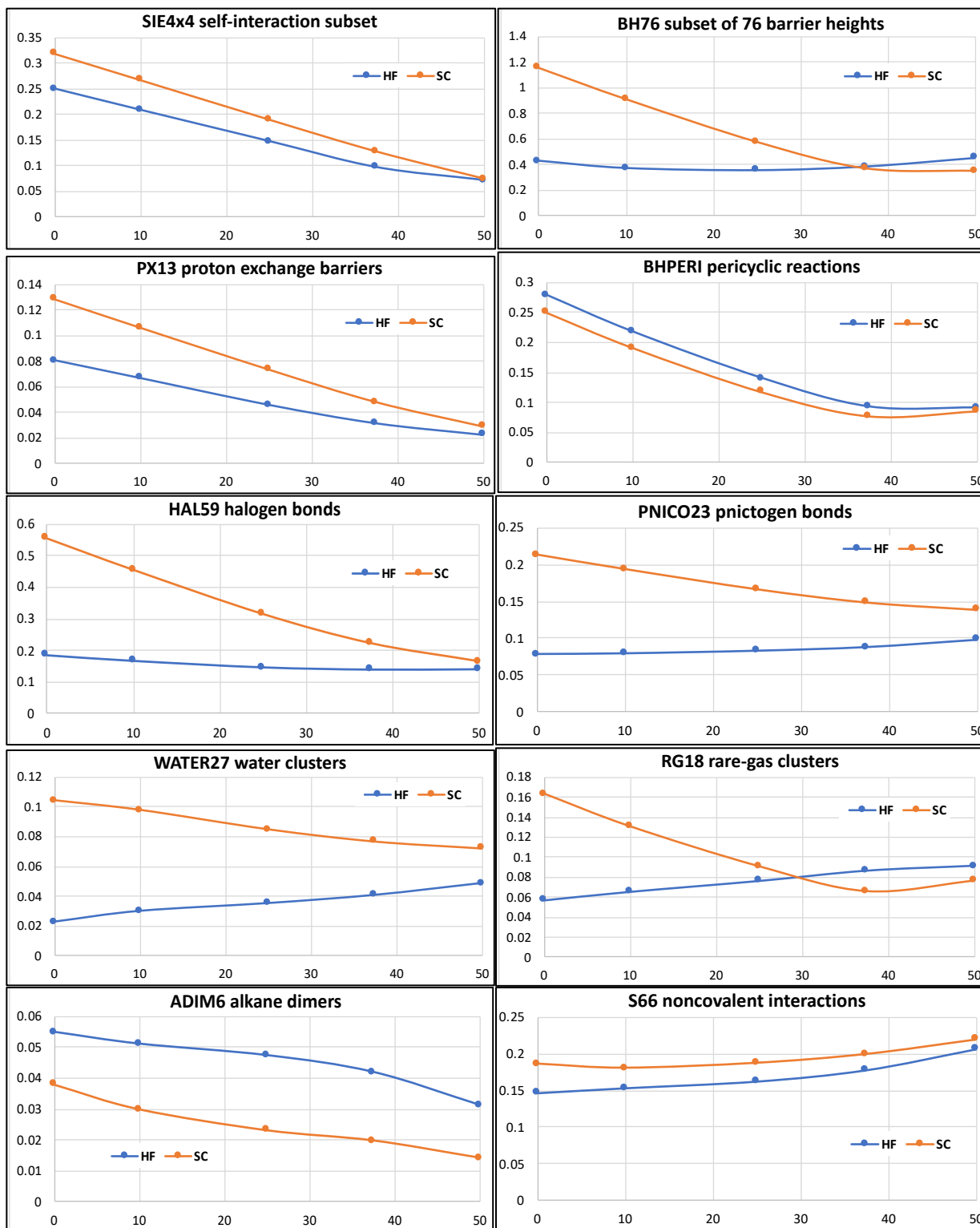


Figure S1: Dependence on the percentage of HF exchange, for self-consistent BnLYP-D4 (SC) and HF-BnLYP-D4 (HF) of the WTMA D2 (kcal/mol) contributions for the individual subsets SIE4x4, BH76, PX13, BHPERI, HAL59, PNICO23, W A TER27, RG18, ADIM6, S66, alkane conformers(ACONF), 1,4-butanediol conformers(BUT14DIOL), oligopeptide conformers(PCONF21), sugar conformers(SCONF), amino acid conformers(AMINO20X4), G21EA, W4-11, DC13 and large molecule isomerization(ISOL24) subsets.



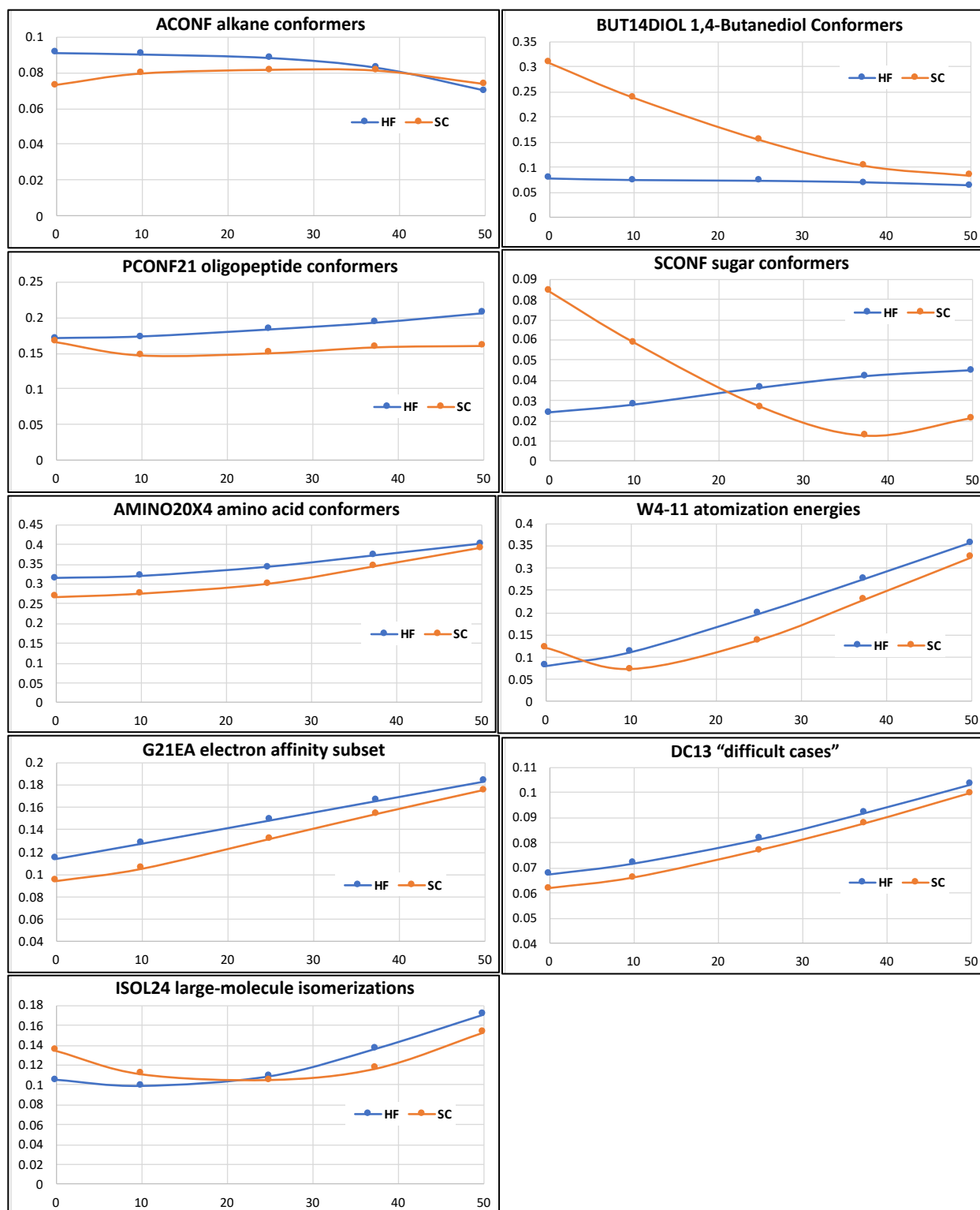


Figure S2: Dependence on the percentage of HF exchange, for self-consistent SCANn-D4 (SC) and HF-SCANn-D4 (HF) of the WTMAD2 (kcal/mol) contributions for the individual subsets SIE4x4, BH76, PX13, BHPERI, HAL59, PNICO23, W A TER27, RG18, ADIM6, S66, alkane

conformers(ACONF), 1,4-butanediol conformers(BUT14DIOL), oligopeptide conformers (PCONF21), sugar conformers(SCONF), amino acid conformers(AMINO20X4), G21EA, W4-11, DC13 and large molecule isomerization(ISOL24) subsets.

HF-DFT

A. Gaussian Sample Inputs:

1. PBE-D3BJ

```
%chk=file.chk  
#p hf nosymm Def2QZVPP guess=save
```

title

```
0 1  
C 0.000000000000 0.000000000000 0.000000000000  
O 0.000000000000 0.000000000000 1.131400000000
```

--Link1--

```
%chk=file.chk  
#p empiricaldispersion=gd3bj pbepbe Def2QZVPP scf(maxcycle=-1)  
geom=allcheck guess=read
```

2. PBE38-D3BJ

```
%chk=file.chk  
%mem=16gb  
#p hf nosymm Def2QZVPP guess=save
```

title

```
0 1  
C 0.000000000000 0.000000000000 0.000000000000  
O 0.000000000000 0.000000000000 1.131400000000
```

--Link1--

```
%chk=file.chk  
#p pbelpbe iop(3/78=1000010000,3/76=0625003750,3/77=1000010000)  
# empiricaldispersion=gd3bj  
iop(3/174=1000000,3/175=1462300,3/177=0399500,3/178=5140500)  
# iop(8/117=-100)
```

```
# scf(maxcycle=-1) chkbas geom=allcheck guess=read
```

B. ORCA Sample input:

1. TPSS-D3BJ

```
! UHF def2-QZVPP def2/J TightSCF NoPop XYZFILE

* xyz 0 1
  C   0.000000000000      0.000000000000      0.000000000000
  O   0.000000000000      0.000000000000      1.131400000000
*

$new_job
! UKS TPSS D3BJ def2-QZVPP def2/J grid5 moread NoPop

%scf
  maxiter 1
  tole 10000
  tolg 10000
end

* xyzfile 0 1
```

2. TPSS38

```
! UHF def2-QZVPP def2/JK TightSCF NoPop XYZFILE

* xyz 0 1
  C   0.000000000000      0.000000000000      0.000000000000
  O   0.000000000000      0.000000000000      1.131400000000
*

$new_job

! UKS TPSS0 def2-QZVPP def2/JK grid5 moread NoPop

%method
  Exchange X_TPSS
  Correlation C_TPSS
  ScalHFX 0.375
  ScalDFX 0.625
  ScalGGAC 1.0000
  ScalLDAC 1.0000
end
```

```
%scf
maxiter 1
tole 10000
tolg 10000
end

* xyzfile 0 1
```

References:

- (1) Gruzman, D.; Karton, A.; Martin, J. M. L. Performance of Ab Initio and Density Functional Methods for Conformational Equilibria of C_nH_{2n+2} Alkane Isomers (n = 4–8) †. *J. Phys. Chem. A* **2009**, *113*, 11974–11983.
- (2) Grimme, S.; Antony, J.; Ehrlich, S.; Krieg, H. A Consistent and Accurate Ab Initio Parametrization of Density Functional Dispersion Correction (DFT-D) for the 94 Elements H-Pu. *J. Chem. Phys.* **2010**, *132*, 154104.
- (3) Lao, K. U.; Schäffer, R.; Jansen, G.; Herbert, J. M. Accurate Description of Intermolecular Interactions Involving Ions Using Symmetry-Adapted Perturbation Theory. *J. Chem. Theory Comput.* **2015**, *11*, 2473–2486.
- (4) Goerigk, L.; Hansen, A.; Bauer, C.; Ehrlich, S.; Najibi, A.; Grimme, S. A Look at the Density Functional Theory Zoo with the Advanced GMTKN55 Database for General Main Group Thermochemistry, Kinetics and Noncovalent Interactions. *Phys. Chem. Chem. Phys.* **2017**, *19*, 32184–32215.
- (5) Yu, H.; Truhlar, D. G. Components of the Bond Energy in Polar Diatomic Molecules, Radicals, and Ions Formed by Group-1 and Group-2 Metal Atoms. *J. Chem. Theory Comput.* **2015**, *11*, 2968–2983.
- (6) Kesharwani, M. K.; Karton, A.; Martin, J. M. L. Benchmark Ab Initio Conformational Energies for the Proteinogenic Amino Acids through Explicitly Correlated Methods. Assessment of Density Functional Methods. *J. Chem. Theory Comput.* **2016**, *12*, 444–454.
- (7) Goerigk, L.; Grimme, S. A General Database for Main Group Thermochemistry, Kinetics, and Noncovalent Interactions – Assessment of Common and Reparameterized (Meta -)GGA Density Functionals. *J. Chem. Theory Comput.* **2010**, *6*, 107–126.
- (8) Zhao, Y.; Lynch, B. J.; Truhlar, D. G. Multi-Coefficient Extrapolated Density Functional Theory for Thermochemistry and Thermochemical Kinetics W. **2005**, 43–52.
- (9) Zhao, Y.; González-García, N.; Truhlar, D. G. Benchmark Database of Barrier Heights for Heavy Atom Transfer, Nucleophilic Substitution, Association, and Unimolecular Reactions and Its Use to Test Theoretical Methods. *J. Phys. Chem. A* **2005**, *109*, 2012–2018.
- (10) Guner, V.; Khuong, K. S.; Leach, A. G.; Lee, P. S.; Bartberger, M. D.; Houk, K. N. A Standard Set of Pericyclic Reactions of Hydrocarbons for the Benchmarking of Computational Methods: The Performance of Ab Initio, Density Functional, CASSCF, CASPT2, and CBS-QB3 Methods for the Prediction of Activation Barriers, Reaction

- Energetics, *And. J. Phys. Chem. A* **2003**, *107*, 11445–11459.
- (11) Ess, D. H.; Houk, K. N. Activation Energies of Pericyclic Reactions: Performance of DFT, MP2, and CBS-QB3 Methods for the Prediction of Activation Barriers and Reaction Energetics of 1,3-Dipolar Cycloadditions, and Revised Activation Enthalpies for a Standard Set of Hydrocarbon. *J. Phys. Chem. A* **2005**, *109*, 9542–9553.
 - (12) Dinadayalane, T. C.; Vijaya, R.; Smitha, A.; Sastry, G. N. Diels–Alder Reactivity of Butadiene and Cyclic Five-Membered Dienes ((CH)₄X, X = CH₂, SiH₂, O, NH, PH, and S) with Ethylene: A Benchmark Study. *J. Phys. Chem. A* **2002**, *106*, 1627–1633.
 - (13) Steinmann, S. N.; Csonka, G.; Corminboeuf, C. Unified Inter- and Intramolecular Dispersion Correction Formula for Generalized Gradient Approximation Density Functional Theory. *J. Chem. Theory Comput.* **2009**, *5*, 2950–2958.
 - (14) Krieg, H.; Grimme, S. Thermochemical Benchmarking of Hydrocarbon Bond Separation Reaction Energies: Jacob’s Ladder Is Not Reversed! *Mol. Phys.* **2010**, *108*, 2655–2666.
 - (15) Kozuch, S.; Bachrach, S. M.; Martin, J. M. L. Conformational Equilibria in Butane-1,4-Diol: A Benchmark of a Prototypical System with Strong Intramolecular H-Bonds. *J. Phys. Chem. A* **2014**, *118*, 293–303.
 - (16) Sure, R.; Hansen, A.; Schwerdtfeger, P.; Grimme, S. Comprehensive Theoretical Study of All 1812 C₆₀isomers. *Phys. Chem. Chem. Phys.* **2017**, *19*, 14296–14305.
 - (17) Yu, L.-J.; Karton, A. Assessment of Theoretical Procedures for a Diverse Set of Isomerization Reactions Involving Double-Bond Migration in Conjugated Dienes. *Chem. Phys.* **2014**, *441*, 166–177.
 - (18) Johnson, E. R.; Mori-Sánchez, P.; Cohen, A. J.; Yang, W. Delocalization Errors in Density Functionals and Implications for Main-Group Thermochemistry. *J. Chem. Phys.* **2008**, *129*, 204112.
 - (19) Zhao, Y.; Truhlar, D. G. The M06 Suite of Density Functionals for Main Group Thermochemistry, Thermochemical Kinetics, Noncovalent Interactions, Excited States, and Transition Elements: Two New Functionals and Systematic Testing of Four M06-Class Functionals and 12 Other Function. *Theor. Chem. Acc.* **2008**, *120*, 215–241.
 - (20) Grimme, S. Semiempirical Hybrid Density Functional with Perturbative Second-Order Correlation. *J. Chem. Phys.* **2006**, *124*, 034108.
 - (21) Grimme, S.; Mück-Lichtenfeld, C.; Würthwein, E. U.; Ehlers, A. W.; Goumans, T. P. M.; Lammertsma, K. Consistent Theoretical Description of 1,3-Dipolar Cycloaddition Reactions. *J. Phys. Chem. A* **2006**, *110*, 2583–2586.
 - (22) Piacenza, M.; Grimme, S. Systematic Quantum Chemical Study of DNA-Base Tautomers. *J. Comput. Chem.* **2004**, *25*, 83–98.
 - (23) Woodcock, H. L.; Schaefer, H. F.; Schreiner, P. R. Problematic Energy Differences between Cumulenes and Poly-Ynes: Does This Point to a Systematic Improvement of Density Functional Theory? *J. Phys. Chem. A* **2002**, *106*, 11923–11931.
 - (24) Schreiner, P. R.; Fokin, A. A.; Pascal, R. A.; de Meijere, A. Many Density Functional Theory Approaches Fail To Give Reliable Large Hydrocarbon Isomer Energy Differences. *Org. Lett.* **2006**, *8*, 3635–3638.
 - (25) Lepetit, C.; Chermette, H.; Heully, J.; Lyon, D.; Uni, V.; Umr, C. Description of Carbo - Oxocarbons and Assessment of Exchange-Correlation Functionals for the DFT Description of Carbo -Mers. **2007**, 136–149.
 - (26) Lee, J. S. Accurate Ab Initio Binding Energies of Alkaline Earth Metal Clusters. *J. Phys. Chem. A* **2005**, *109*, 11927–11932.

- (27) Karton, A.; Martin, J. M. L. Explicitly Correlated Benchmark Calculations on C₈H₈ Isomer Energy Separations: How Accurate Are DFT, Double-Hybrid, and Composite Ab Initio Procedures? *Mol. Phys.* **2012**, *110*, 2477–2491.
- (28) Zhao, Y.; Tishchenko, O.; Gour, J. R.; Li, W.; Lutz, J. J.; Piecuch, P.; Truhlar, D. G. Thermochemical Kinetics for Multireference Systems: Addition Reactions of Ozone. *J. Phys. Chem. A* **2009**, *113*, 5786–5799.
- (29) Manna, D.; Martin, J. M. L. What Are the Ground State Structures of C₂₀ and C₂₄? An Explicitly Correlated Ab Initio Approach. **2016**.
- (30) Friedrich, J.; Hänchen, J. Incremental CCSD(T)(F12*)/MP2: A Black Box Method To Obtain Highly Accurate Reaction Energies. *J. Chem. Theory Comput.* **2013**, *9*, 5381–5394.
- (31) Friedrich, J. Efficient Calculation of Accurate Reaction Energies - Assessment of Different Models in Electronic Structure Theory. *J. Chem. Theory Comput.* **2015**, *11*, 3596–3609.
- (32) Curtiss, L. A.; Raghavachari, K.; Trucks, G. W.; Pople, J. A. Gaussian-2 Theory for Molecular Energies of First- and Second-row Compounds. *J. Chem. Phys.* **1991**, *94*, 7221–7230.
- (33) Curtiss, L. A.; Raghavachari, K.; Redfern, P. C.; Pople, J. A. Assessment of Gaussian-2 and Density Functional Theories for the Computation of Enthalpies of Formation. *J. Chem. Phys.* **1997**, *106*, 1063–1079.
- (34) Kozuch, S.; Martin, J. M. L. Halogen Bonds: Benchmarks and Theoretical Analysis. *J. Chem. Theory Comput.* **2013**, *9*, 1918–1931.
- (35) Řezáč, J.; Riley, K. E.; Hobza, P. Benchmark Calculations of Noncovalent Interactions of Halogenated Molecules. *J. Chem. Theory Comput.* **2012**, *8*, 4285–4292.
- (36) Schwabe, T.; Grimme, S. Double-Hybrid Density Functionals with Long-Range Dispersion Corrections: Higher Accuracy and Extended Applicability. *Phys. Chem. Chem. Phys.* **2007**, *9*, 3397–3406.
- (37) Grimme, S. Seemingly Simple Stereoelectronic Effects in Alkane Isomers and the Implications for Kohn–Sham Density Functional Theory. *Angew. Chemie Int. Ed.* **2006**, *45*, 4460–4464.
- (38) Goerigk, L.; Grimme, S. Efficient and Accurate Double-Hybrid-Meta-GGA Density Functionals—Evaluation with the Extended GMTKN30 Database for General Main Group Thermochemistry, Kinetics, and Noncovalent Interactions. *J. Chem. Theory Comput.* **2011**, *7*, 291–309.
- (39) Grimme, S.; Steinmetz, M.; Korth, M. How to Compute Isomerization Energies of Organic Molecules with Quantum Chemical Methods. *J. Org. Chem.* **2007**, *72*, 2118–2126.
- (40) Goerigk, L.; Sharma, R. The INV24 Test Set: How Well Do Quantum-Chemical Methods Describe Inversion and Racemization Barriers? *Can. J. Chem.* **2016**, *94*, 1133–1143.
- (41) Huenerbein, R.; Schirmer, B.; Moellmann, J.; Grimme, S. Effects of London Dispersion on the Isomerization Reactions of Large Organic Molecules: A Density Functional Benchmark Study. *Phys. Chem. Chem. Phys.* **2010**, *12*, 6940.
- (42) Fogueri, U. R.; Kozuch, S.; Karton, A.; Martin, J. M. L. The Melatonin Conformer Space: Benchmark and Assessment of Wave Function and DFT Methods for a Paradigmatic Biological and Pharmacological Molecule. *J. Phys. Chem. A* **2013**, *117*, 2269–2277.
- (43) Grimme, S.; Kruse, H.; Goerigk, L.; Erker, G. The Mechanism of Dihydrogen Activation

- by Frustrated Lewis Pairs Revisited. *Angew. Chemie Int. Ed.* **2010**, *49*, 1402–1405.
- (44) Setiawan, D.; Kraka, E.; Cremer, D. Strength of the Pnictogen Bond in Complexes Involving Group Va Elements N, P, and As. *J. Phys. Chem. A* **2015**, *119*, 1642–1656.
- (45) Karton, A.; O'Reilly, R. J.; Chan, B.; Radom, L. Determination of Barrier Heights for Proton Exchange in Small Water, Ammonia, and Hydrogen Fluoride Clusters with G4(MP2)-Type, MPn, and SCS-MPn Procedures—a Caveat. *J. Chem. Theory Comput.* **2012**, *8*, 3128–3136.
- (46) Neese, F.; Schwabe, T.; Kossmann, S.; Schirmer, B.; Grimme, S. Assessment of Orbital-Optimized, Spin-Component Scaled Second-Order Many-Body Perturbation Theory for Thermochemistry and Kinetics. *J. Chem. Theory Comput.* **2009**, *5*, 3060–3073.
- (47) Jurečka, P.; Šponer, J.; Černý, J.; Hobza, P. Benchmark Database of Accurate (MP2 and CCSD(T) Complete Basis Set Limit) Interaction Energies of Small Model Complexes, DNA Base Pairs, and Amino Acid Pairs. *Phys. Chem. Chem. Phys.* **2006**, *8*, 1985–1993.
- (48) Rezáč, J.; Riley, K. E.; Hobza, P. S66: A Well-Balanced Database of Benchmark Interaction Energies Relevant to Biomolecular Structures. *J. Chem. Theory Comput.* **2011**, *7*, 2427–2438.
- (49) Csonka, G. I.; French, A. D.; Johnson, G. P.; Stortz, C. A. Evaluation of Density Functionals and Basis Sets for Carbohydrates. *J. Chem. Theory Comput.* **2009**, *5*, 679–692.
- (50) Karton, A.; Rabinovich, E.; Martin, J. M. L.; Ruscic, B. W4 Theory for Computational Thermochemistry: In Pursuit of Confident Sub-KJ/Mol Predictions. *J. Chem. Phys.* **2006**, *125*, 144108.
- (51) Kruse, H.; Mladek, A.; Gkionis, K.; Hansen, A.; Grimme, S.; Sponer, J. Quantum Chemical Benchmark Study on 46 RNA Backbone Families Using a Dinucleotide Unit. *J. Chem. Theory Comput.* **2015**, *11*, 4972–4991.
- (52) Karton, A.; Daon, S.; Martin, J. M. L. W4-11: A High-Confidence Benchmark Dataset for Computational Thermochemistry Derived from First-Principles W4 Data. *Chem. Phys. Lett.* **2011**, *510*, 165–178.
- (53) Bryantsev, V. S.; Diallo, M. S.; van Duin, A. C. T.; Goddard, W. A. Evaluation of B3LYP, X3LYP, and M06-Class Density Functionals for Predicting the Binding Energies of Neutral, Protonated, and Deprotonated Water Clusters. *J. Chem. Theory Comput.* **2009**, *5*, 1016–1026.
- (54) Karton, A.; O'Reilly, R. J.; Radom, L. Assessment of Theoretical Procedures for Calculating Barrier Heights for a Diverse Set of Water-Catalyzed Proton-Transfer Reactions. *J. Phys. Chem. A* **2012**, *116*, 4211–4221.
- (55) Zhao, Y.; Ng, H. T.; Peverati, R.; Truhlar, D. G. Benchmark Database for Ylidic Bond Dissociation Energies and Its Use for Assessments of Electronic Structure Methods. *J. Chem. Theory Comput.* **2012**, *8*, 2824–2834.
- (56) Caldeweyher, E.; Ehlert, S.; Hansen, A.; Neugebauer, H.; Spicher, S.; Bannwarth, C.; Grimme, S. A Generally Applicable Atomic-Charge Dependent London Dispersion Correction. *J. Chem. Phys.* **2019**, *150*, 154122.
- (57) Caldeweyher, E.; Bannwarth, C.; Grimme, S. Extension of the D3 Dispersion Coefficient Model. *J. Chem. Phys.* **2017**, *147*, 034112.